Behavioral/Cognitive

Identified Serotonin-Releasing Neurons Induce Behavioral Quiescence and Suppress Mating in *Drosophila*

Atefeh Pooryasin and André Fiala

Georg-August-University Göttingen, Johann-Friedrich-Blumenbach-Institute for Zoology and Anthropology, Department of Molecular Neurobiology of Behavior, 37077 Göttingen, Germany

Animals show different levels of activity that are reflected in sensory responsiveness and endogenously generated behaviors. Biogenic amines have been determined to be causal factors for these states of arousal. It is well established that, in *Drosophila*, dopamine and octopamine promote increased arousal. However, little is known about factors that regulate arousal negatively and induce states of quiescence. Moreover, it remains unclear whether global, diffuse modulatory systems comprehensively affecting brain activity determine general states of arousal. Alternatively, individual aminergic neurons might selectively modulate the animals' activity in a distinct behavioral context. Here, we show that artificially activating large populations of serotonin-releasing neurons induces behavioral quiescence and inhibits feeding and mating. We systematically narrowed down a role of serotonin in inhibiting endogenously generated locomotor activity to neurons located in the posterior medial protocerebrum. We identified neurons of this cell cluster that suppress mating, but not feeding behavior. These results suggest that serotonin does not uniformly act as global, negative modulator of general arousal. Rather, distinct serotoninergic neurons can act as inhibitory modulators of specific behaviors.

Key words: arousal; *Drosophila*; motivational behavior; neuronal circuits; serotonin; thermogenetics

---

Significance Statement

An animal's responsiveness to external stimuli and its various types of endogenously generated, motivated behavior are highly dynamic and change between states of high activity and states of low activity. It remains unclear whether these states are mediated by unitary modulatory systems globally affecting brain activity, or whether distinct neurons modulate specific neuronal circuits underlying particular types of behavior. Using the model organism *Drosophila melanogaster*, we find that activating large proportions of serotonin-releasing neurons induces behavioral quiescence. Moreover, distinct serotonin-releasing neurons that we genetically isolated and identified negatively affect aspects of mating behavior, but not food uptake. This demonstrates that individual serotoninergic neurons can modulate distinct types of behavior selectively.

Introduction

An animal's responsiveness to external stimuli and its endogenously generated behavior are highly dynamic and change from

states of drowsiness to states of vigilance. The behavioral diversity of this phenomenon, which can be found across the spectrum of sensory modalities and behaviors, is known generally as "central arousal" (Hebb, 1955; Andrew, 1974; Coull, 1998; Pfaff et al., 2008). A prominent reflection of dynamic arousal states is found in sleep–wake behavior controlled by circadian pacemaker neurons, external sensory signals, and homeostatic sleep needs (Brown et al., 2012). However, states of low or high arousal are also reflected in the variability of many complex behavioral classes influenced by motivational factors (e.g., mating or feeding). The neuronal mechanisms that determine the dynamics of arousal states are unclear. In particular, the question of whether a unitary factor (e.g., a neuromodulatory substance or a dedicated neuronal circuitry) governs a general, central arousal state, or whether distinct subsystems influence behavior-specific aspects of arousal independently (Pfaff et al., 2008; Jing et al., 2009; Leb-

estky et al., 2009; Van Swinderen and Andretic, 2011) remains unanswered as yet.

Drosophila represents a favorable model organism to dissect neuronal circuits genetically and to manipulate the activity of defined neuronal populations experimentally (Venken et al., 2011). In *Drosophila*, dopamine (DA) and octopamine have been identified as arousal-increasing signals (Andretic et al., 2005; Kume et al., 2005; Crocker et al., 2010; Liu et al., 2012b; Ueno et al., 2012), when analyzed comprehensively as unitary modulatory systems. In addition, different forms of arousal (i.e., "endogenous" arousal), as defined by self-generated locomotor activity periods, and exogenous, startle-induced arousal, are differently affected by mutating one dopamine receptor (Lebestky et al., 2009). However, whether antagonistic modulatory systems exist that downregulate the animals' activity and responsiveness (i.e., that induce behavioral quiescence) remains unknown. Here we found that thermogenetic depolarization of the majority of serotoninergic (5-HT) neurons, mediated by the temperature-sensitive cation channel, dTRPA1 (Hamada et al., 2008), suppresses endogenously generated locomotion activity independently of the animals' ability to move. This inhibition of locomotion activity was accompanied by a decline in feeding and mating behavior. We were puzzled by the question of whether 5-HT acts as a diffuse, global control signal over brain activity, thereby affecting multiple types of behavior in general, or whether distinct 5-HT neurons modulate specific behavioral classes selectively. To clarify this, we used stochastic transgene expression and intersectional genetics to isolate neurons among the plethora of 5-HT neurons that mediate an overall decrease in locomotion behavior. We identified a specific subgroup of 5-HT neurons located ventrally in the posterior medial protocerebral (PMPV) cluster that inhibits endogenously generated locomotor activity and also mating behavior. However, feeding behavior remained unaffected by these neurons; this demonstrates the existence of distinct neuronal elements negatively regulating selective, behavior-specific aspects of arousal.

Materials and Methods

Generation of DNA constructs and transgenic flies. Flies expressing two copies of flippase separated by an IRES sequence (FIF) and carrying a SV40 sequence at the 3′ end (Bohm et al., 2010) under direct control of the tyrosine hydroxylase (Trh) promoter sequence (Alekseyenko et al., 2010) were generated by amplifying the FIF DNA construct (provided by Bing Zhang) using the linker primers 5′-GGACGCGTTGCACGTTTG CTTGTTGAGAG-3′ and 5′-CCACCGGTGATGAGTTTGGACAAACC ACA-3′ and the Trh promoter sequence (provided by Edward Kravitz) using the linker primers 5′-TACGTACGATAAAAGTAAATATCTGG TAC-3′ and 5′-ATGCATGCCTTGGTAGCTACTCGTTTTCG-3′. Both constructs were inserted into a modified backbone of the pBDP vector (Pfeiffer et al., 2008). The detailed pBDP backbone modification is available upon request. Germ line transformation was performed by BestGene.

Fly strains. All flies were reared on standard corn meal medium at 60% humidity and a 12 h/12 h light-dark cycle. Flies used for thermogenetic experiments were raised at 18°C; otherwise, flies were raised at 25°C. Wild-type flies were of the Canton-S strain, obtained from the Bloomington Stock Center. Trh-Gal4 strains were kindly provided by Jaeseob Kim (Park et al., 2006), Serge Birman (Sitaraman et al., 2012), and Edward Kravitz (Alekseyenko et al., 2010). Furthermore, the following fly strains were used: Ddc-Gal4 (Li et al., 2000), D42-Gal4 (Parkes et al., 1998), UAS:dTRPA1-mCherry (Vasmer et al., 2014), UAS:FRT-CD2-stop-FRT-mCherry-dTRPA1 (Vasmer et al., 2014), 20xUAS:shibire[(ts)] (Pfeiffer et al., 2012), UAS:dicer2 (Dietzl et al., 2007), UAS:Trh-RNAi, JF01863 (TRiP collection) (Ni et al., 2009), UAS:mCD8-GFP (Pfeiffer et al., 2010), UAS:FRT-stop-FRT-mCD8:GFP (Yu et al., 2010), Tsh-Gal80

(Clyne and Miesenböck, 2008), R58E02-Gal80 (Liu et al., 2012a), hs-FLP (Basler and Struhl, 1994), Actin-FRT-stop-FRT-Gal4; UAS:GFP (Pignoni and Zipursky, 1997), and UAS:Flybow 2.0 and m-hs-FLP (Hadjieconomou et al., 2011; Shimosako et al., 2014). The following Gal4 driver lines from the Janelia Farm Gal4 collection (Jenett et al., 2012) were obtained from the Bloomington Stock Center: R66A09-Gal4, R67B05-Gal4, R70A11-Gal4, R23E12-Gal4, R75D10-Gal4, R65D03-Gal4, and R35C08-Gal4.

Immunohistochemistry. Brains and thoracic/abdominal ganglia were dissected in Ringer's solution (pH 7.3, 290–310 mOsm) containing 5 mM HEPES-NaOH, 130 mM NaCl, 5 mM KCl, 2 mM MgCl$_2$, 2 mM CaCl$_2$, and 36 mM sucrose, fixed in 4% PFA for 2 h at 4°C and washed three times for 10 min each in PBS containing 0.6% Triton X-100 (PBT) at room temperature. Samples were incubated for 2 h in PBT containing 2% BSA and 5% normal goat serum. Subsequently, the samples were incubated in the primary antibody diluted in block solution at 4°C overnight. Samples were washed three times for at least 30 min each in PBT containing 2% BSA (PAT) at room temperature, subsequently incubated with secondary antibodies diluted in PAT for 4 h at room temperature or overnight at 4°C, washed at least six times for 30 min each in PBT and embedded in Vectashield (Vector Laboratories). The following antibodies were used: For staining mCherry-dTRPA1, rat anti-RFP (Chromotek, 5F8, diluted 1: 350) and AlexaFluor-488-coupled goat anti-rat (Invitrogen, A11006, diluted 1:300) or Cy3-coupled goat anti rat (Invitrogen, A10522, diluted 1:500) were used. For staining GFP, mouse anti-GFP (Invitrogen, A11120, diluted 1: 750) or rabbit anti-GFP (Invitrogen, A6455, diluted 1:750) and AlexaFluor-488-coupled goat anti-mouse (Invitrogen, A11001, diluted 1:200) or AlexaFluor-488-coupled goat anti-rabbit (Invitrogen, A11034, diluted 1:300) were used. For staining 5-HT, rabbit anti-5-HT (Sigma, S5545, diluted 1:500) and AlexaFluor-633-coupled goat anti-rabbit (Invitrogen, A21070, diluted 1:500) were used. For detecting stochastically expressed mCherry-dTRPA1, the biotin-streptavidin system was used to enhance signal intensity. As primary antibodies, a mixture of rat anti-RFP and anti-5-HT was used, as described above. After washing the samples at least three times for 30 min each at room temperature, they were incubated in biotin-coupled goat anti-rat antibody (Invitrogen, 62-9540, diluted 1:200 in block solution) for 3 h at room temperature. Samples were washed three times for 30 min each in PAT at room temperature, and a mixture of streptavidin-coupled AlexaFluor-488 (Invitrogen, S11223, diluted 1:300) and AlexaFluor-633-coupled goat anti-rabbit antibody (Invitrogen, A21070, diluted 1:300) was subsequently used. For the flybow technique, rabbit anti-5-HT (Sigma, S5545, diluted 1:500) and mouse anti-DLG (DSHB, diluted 1:200) as primary antibodies, and Cy5-coupled goat anti-rabbit (Invitrogen, A10523, diluted 1:300) and Cy3-coupled goat anti-mouse (Jackson ImmunoResearch Laboratories, 115-165-003, diluted 1:300), as secondary antibodies, were used.

Confocal imaging and data processing. Immunostained samples were analyzed using either a Leica TC SP2 or a SP8 confocal microscope equipped with a 20 × Leica apochromat water-immersion objective (NA = 0.7) or a Leica apochromat 20× glycerol-immersion objective (NA = 0.75). AlexaFluor-488 was excited at 488 nm, Cy3 at 543 nm, and Alexa-633 at 633 nm wavelengths. Samples were scanned at 1 μm sections in the z direction with a frame average of 4 and a resolution of 0.57 μm/pixel. All images were acquired at 8-bit or 12-bit grayscale. For comparing the intensity of anti-5-HT staining across different samples, a Zeiss LSM7 MP two-photon microscope equipped with a 20× Zeiss w-plan aprochromat water-immersion objective (NA = 1.0) was used. Images were acquired at 920 nm excitation wavelength, with a frame average of 4, at 1 μm steps in the z-direction and a resolution of 0.6 μm/pixel. Images were processed using the Fiji software (Schindelin et al., 2012) for adjusting brightness, merging of two emission channels and calculating maximal intensity projections across the z-axis. For the flybow technique, all images were obtained with a Leica TCS SP8 confocal microscope and a Leica apochromat 20× glycerol-immersion objective (NA = 0.75). EGFP was excited at 488 nm, mCitrin at 514 nm, Cy3 at 561 nm, and Cy5 at 633 nm wavelengths. The images were acquired with a frame average of 4, at 1 μm steps in the z-direction and at a resolution of
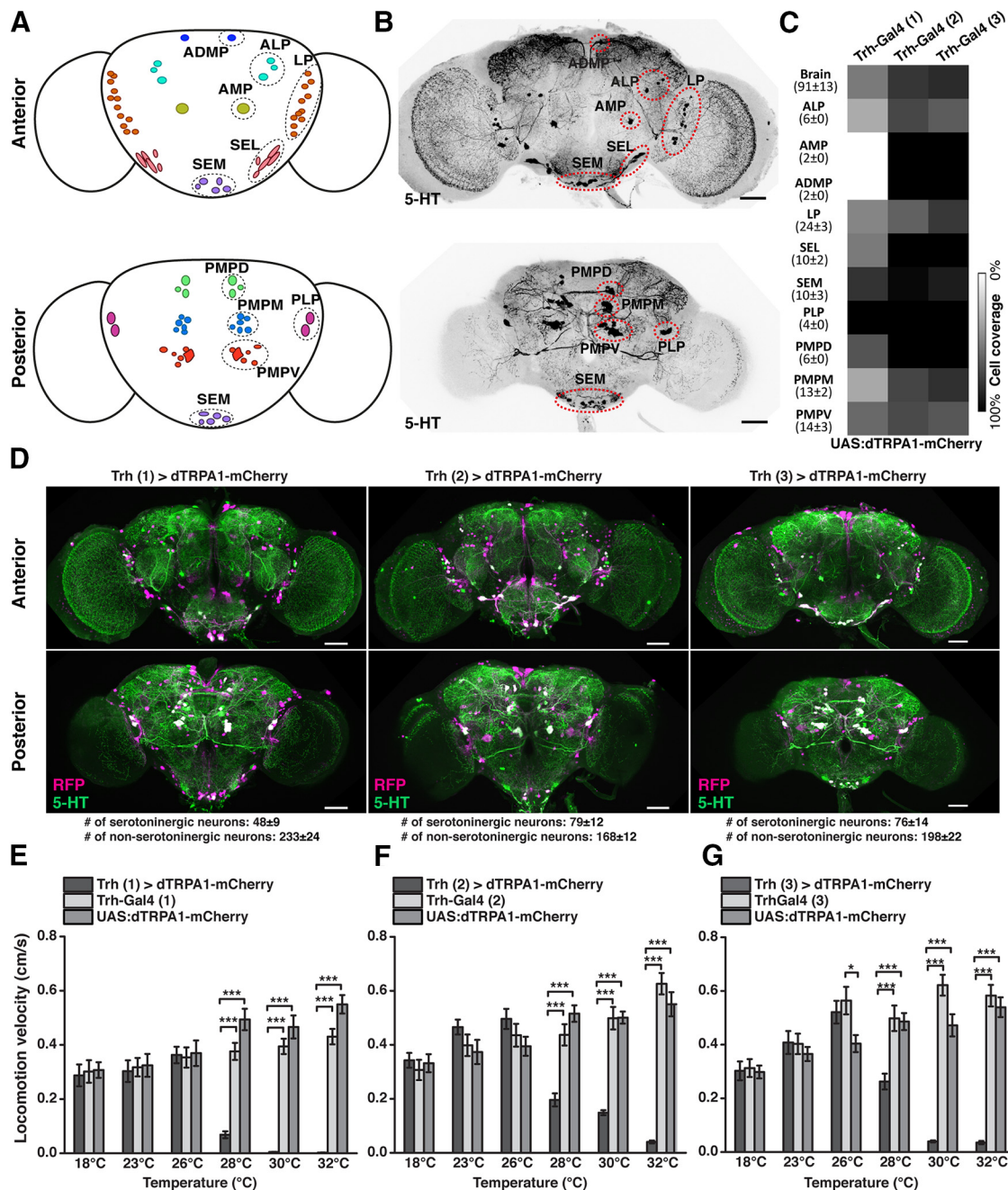
Figure 1. Thermogenetic activation of Trh-Gal4-positive neurons induces behavioral quiescence. *A*, Schematic illustration of 5-HT neuron clusters in the central brain. *B*, 5-HT-immunoreactive neurons in the brain. *C*, Coverage of 5-HT neurons by three different Trh-Gal4 strains. Numbers in parentheses indicate the total numbers of 5-HT-immunoreactive neurons for each cluster in both central brain hemispheres (mean $\pm$ SD, $n = 18$). Grayscale represents the relative coverage of these neurons by the three Trh-Gal4 lines when UAS:dTRPA1-mCherry is used as a reporter ($n = 3$ brains each). *D*, Expression of dTRPA1-mCherry under control of the three Trh-Gal4 lines. Magenta represents anti-RFP immunostaining against dTRPA1-mCherry. Green represents anti-5-HT immunostaining. White represents the overlap. Images represent maximal intensity *z*-axis projections across stacks of confocal images. The numbers of somata are indicated below the panels (mean $\pm$ SD, $n = 3$ brains). *E–G*, Temperature-dependent decrease in locomotion velocity in flies expressing dTRPA1-mCherry under control of the three Trh-Gal4 lines compared with the heterozygous Trh-Gal4 lines and the heterozygous UAS:dTRPA1-mCherry line. Bars indicate mean $\pm$ SEM ($n = 27$ each). *$p < 0.05$. ***$p < 0.001$. For exact statistical values, see Table 3. Scale bars, 50 μm.

0.39 μm/pixel. For 3D reconstructions, the Amira 5.3.3 software (FEI) was used.

Pharmacological treatment. Female flies (3- to 4-d-old) were starved for 48 h at 18°C and transferred to a vial containing 1 ml standard corn meal medium mixed with 60 mg para-chlorphenylalanin (Sigma), 200 μl 5% sucrose solution, 200 μl tap water, and 15 μl red food coloring (Ruth) for 4 d at 25°C.

Locomotor activity assay. Locomotion activity was quantified using a custom-made apparatus consisting of an aluminum plate divided into 10

"walking arenas" (29 $\times$ 0.5 $\times$ 0.4 cm), covered with Plexiglas, and equipped with an internal temperature sensor. Locomotor activity of female flies transferred into the arenas without anesthesia was recorded for 10 min using a CCD camera (DCR-SR57, Sony). Experiments were performed under constant red light conditions, relative humidity of 60%, and controlled temperature that depended on the experiment. Locomotor activity was analyzed using the video tracking software, Etho-Vision XT 8.5 (Noldus), which distinguishes the animals and their movements from background and registers the animals' *x*/*y* coordinates

at a rate of 1 Hz. By calibrating the movies and the coordinates to the size of the walking arenas, movement velocity was calculated as cm/s. For experiments involving shibire[(ts)] or Trh-RNAi, the animals were kept at 32°C for 10 min before testing.

Electric shock avoidance assay. Shock avoidance was measured in a T-maze apparatus consisting of a "shock tube" equipped with a copper grid and a "safe tube." Groups of 50–60 flies were placed in the shock tube, and 12 electric shocks of 90 V (1.25 s shock with 3.75 s interpulse interval) were applied. The flies were allowed to escape from the shock tube for 1 min. The experiment was performed at either 22°C or 32°C. After counting the flies on each side of the T-maze a shock avoidance index (SI) was calculated as follows: SI (%) = (number of flies in the safe tube/total number of flies) × 100.

Forced flight assay. Using a funnel, groups of ~100 flies were tapped into a 500 ml graduated cylinder (50 mm diameter), whose wall was coated inside with paraffin oil. Flies that reflexively started flying got trapped in the oil. The cylinder was divided into two halves and a forced flight index (FI) was calculated according to Wagh et al. (2006) as follows: FI (%) = (number of flies stuck to the upper half of the cylinder/total number of flies) × 100. The experiment was performed at either 22°C or 32°C.

Negative geotaxis assay. Negative geotaxis behavior was quantified according to Benzer et al. (1967) using a modified assay described by Inagaki et al. (2010).

Courtship behavior assay. Pairs of virgin male and female flies (5- to 6-d-old) were transferred to the wells of an 8-well cell culture plate (each well 15.2 mm in diameter, 10 mm in height) covered by a Plexiglas lid. Experiments were conducted at either 18°C or 29°C and 55%–65% humidity. Courtship behavior was recorded for 10 min using a CCD camera (DCR-SR57, Sony). A courtship index was calculated as the total amount of time a male was engaged in courtship activity divided by the total time or the time until copulation (Siegel and Hall, 1979). Male wing extension frequency was determined by counting the number of wing extensions toward a female, copulation attempt frequency as the number of abdomen bends oriented behind the female, and copulation latency as the time until copulation.

Food uptake assay. Female flies (3- to 4-d-old) were starved for 48 h at 18°C, transferred to food vials containing 5 ml 50% fluid, red food coloring (Ruth), 0.5% agarose, and 0.5 M sucrose, and were allowed to feed for 45 min at 18°C or 32°C. Subsequently, 20 flies were decapitated, the bodies were collected in 2 ml microcentrifuge tubes, homogenized in 500 μl distilled water, and centrifuged for 1 min at 13,000 rpm. Three 100 μl samples of supernatant from each probe were taken, and absorbance of red dye was quantified using a 96-well microplate spectrophotometer at 500 nm. The three values were averaged; and the absorbance values for flies treated equivalently, but without feeding on red food coloring, were subtracted.

Proboscis extension reflex assay. Female flies (3- to 4-d-old) were starved for 48 h at 18°C. Individual flies were gently inserted into a 200 μl pipette tip without anesthesia. To expose the proboscis, the pipette tip was cut in front of the head; the fly's head was pushed out of the tip and fixed using modeling clay (Shiraiwa and Carlson, 2007). The experiment was conducted at 18°C or 32°C and 60%–70% humidity. The proboscis extension reflex of each fly was tested by stimulating the proboscis with water and with increasing concentrations of sucrose (10 mM to 1 M).

Circadian rhythm and sleep assay. Locomotion activity over a period of 3 d was measured using the Drosophila Activity Monitor System (Trikinetics) (Pfeiffenberger et al., 2010). Thirty-two individual female flies were placed in glass tubes containing a food source at one end and were allowed to adjust to the environment for 1 d before the experiment. Their movements were detected by the interruption of an infrared beam at the center of the tube. The number of interruptions per minute was counted and analyzed using an Excel Visual Basic Application. The Drosophila Activity Monitor System was positioned in an incubator with controlled 12 h/12 h light-dark cycle, constant relative humidity of 60%, and controlled ambient temperature that depended on the experiment. Sleep was defined as any period of inactivity longer than 5 min, according to Shaw et al. (2000).

Statistical analysis. Data were tested for normal distribution using the Shapiro–Wilk test. For testing for differences between two normally dis-

Table 1. Nomenclature of 5-HT neuron clusters according to the location of somata compared with previous studies

5-HT cluster	Location	Vallés and White (1988)	Sitaraman et al. (2012)
ALP	Anterior lateral protocerebrum	—	ALP
AMP	Anterior medial protocerebrum	—	AMP
ADMP	Anterior dorsomedial protocerebrum	—	—
LP	Lateral protocerebrum	LP2a,b	LP2
SEL	Lateral subesophageal ganglion	SE1 and SE2	SE1 and SE2
SEM	Medial subesophageal ganglion	SE3	SE3
PLP	Posterior lateral protocerebrum	LP1	PLP
PMPD	Posterior medial protocerebrum, dorsal	SP1	PMP
PMPM	Posterior medial protocerebrum, medial	SP2	PMP
PMPV	Posterior medial protocerebrum, ventral	IP	PMP

Table 2. Quantification of serotoninergic and nonserotoninergic neurons in the central brain expressing dTRPA1-mCherry under control of three different Trh-Gal4 lines[a]

5-HT cell cluster	5-HT-positive	Trh-Gal4 (1) (Park et al., 2006)	Trh-Gal4 (2) (Sitaraman et al., 2012)	Trh-Gal4 (3) (Alekseyenko et al., 2010)
ALP	6 ± 0	2 ± 0	4 ± 1	4 ± 1
AMP	2 ± 0	0 ± 0	2 ± 0	2 ± 0
ADMP	2 ± 0	0 ± 0	2 ± 0	2 ± 0
LP	24 ± 3	11 ± 1	19 ± 3	18 ± 3
SEL	10 ± 2	5 ± 1	12 ± 0	11 ± 1
SEM	10 ± 3	8 ± 2	8 ± 3	9 ± 3
PLP	4 ± 0	4 ± 0	4 ± 0	4 ± 0
PMPD	6 ± 0	4 ± 0	6 ± 0	6 ± 0
PMPM	13 ± 2	5 ± 2	10 ± 3	12 ± 3
PMPV	14 ± 3	9 ± 3	10 ± 2	8 ± 3
∑ 5-HT neurons	91 ± 13	48 ± 9	79 ± 12	76 ± 14
Non-5-HT neurons		233 ± 24	168 ± 12	198 ± 22

[a]The number of serotoninergic (5-HT-positive) neurons and nonserotoninergic cells in each identified neuron cluster of the central brain (i.e., excluding the optical lobes) covered by Trh-Gal4 (1), Trh-Gal4 (2), and Trh-Gal4 (3) are indicated as mean ± SD (n = 3 brains, both hemispheres). The references indicate the description of the respective Gal4 lines.

tributed groups of data, the Student's *t* test was used. For testing for differences among multiple groups of normally distributed data, one-way ANOVA with *post hoc* Bonferroni tests was used. For nonparametric data, the Mann–Whitney *U* test (two groups) or the Kruskal–Wallis test (multiple groups) with pairwise *post hoc* comparisons was used. Fisher's exact test was used for comparing binomially distributed data. Multiple regression analysis with Bonferroni correction was performed using the Statistica software (Statsoft).

Results

Thermogenetic activation of 5-HT-releasing neurons induces behavioral inactivity

The *Drosophila* central brain is extensively innervated by ~90 5-HT-releasing neurons whose somata are grouped in stereotypically localized, identified clusters (Vallés and White, 1988; Alekseyenko et al., 2010; Sitaraman et al., 2012; Pech et al., 2013) (Fig. 1A,B; Table 1). As the starting point of a top-down analysis, we first asked whether depolarizing 5-HT neurons en masse would affect the endogenous movement activity of flies. To this end, we used transgenic *Drosophila* strains that express Gal4 under control of promoter sequences of the gene encoding neuronal tryptophan hydroxylase (Trh), a rate-limiting enzyme for the biosynthesis of 5-HT (Coleman and Neckameyer, 2005; Neckameyer et al., 2007). Three *Drosophila* Trh-Gal4 lines have been described, here referred to as Trh-Gal4 (1) (Park et al., 2006), Trh-Gal4 (2) (Sitaraman et al., 2012), and Trh-Gal4 (3) (Alekseyenko et al., 2010). The three Trh-Gal4 lines encompass large

Table 3. Statistical comparisons for temperature-dependent decrease in locomotion velocity, shown in Figure 1E–G[a]

Figure	Temperature (°C)	H (2, N = 81)	p	Multiple pairwise post hoc comparisons	z	p
1E	18	0.496	0.78			
	23	0.261	0.88			
	26	0.251	0.88			
	28	49.940	<0.0001	Trh-Gal4 (1) versus Trh > dTRPA1-mCherry	5.131	<0.0001
				UAS:dTRPA1-mCherry versus Trh > dTRPA1-mCherry	6.773	<0.0001
				UAS:dTRPA1-mCherry versus Trh-Gal4 (1)	1.643	0.30
	30	54.106	<0.0001	Trh-Gal4 (1) versus Trh > dTRPA1-mCherry	5.894	<0.0001
				UAS:dTRPA1-mCherry versus Trh > dTRPA1-mCherry	6.756	<0.0001
				UAS:dTRPA1-mCherry versus Trh-Gal4 (1)	0.862	1.00
	32	57.583	<0.0001	Trh-Gal4 (1) versus Trh > dTRPA1-mCherry	5.298	<0.0001
				UAS:dTRPA1-mCherry versus Trh > dTRPA1-mCherry	7.352	<0.0001
				UAS:dTRPA1-mCherry versus Trh-Gal4 (1)	2.053	0.12
1F	18	1.279	0.53			
	23	5.932	0.052			
	26	4.103	0.129			
	28	34.931	<0.0001	Trh-Gal4 (2) versus Trh > dTRPA1-mCherry	4.130	<0.0001
				UAS:dTRPA1-mCherry versus Trh > dTRPA1-mCherry	5.726	<0.0001
				UAS:dTRPA1-mCherry versus Trh-Gal4 (2)	1.596	0.33
	30	46.979	<0.0001	Trh-Gal4 (2) versus Trh > dTRPA1-mCherry	5.929	<0.0001
				UAS:dTRPA1-mCherry versus Trh > dTRPA1-mCherry	5.940	<0.0001
				UAS:dTRPA1-mCherry versus Trh-Gal4 (2)	0.012	1.00
	32	49.754	<0.0001	Trh-Gal4 (2) versus Trh > dTRPA1-mCherry	6.478	<0.001
				UAS:dTRPA1-mCherry versus Trh > dTRPA1-mCherry	5.651	<0.001
				UAS:dTRPA1-mCherry versus Trh-Gal4 (2)	0.827	1.00
1G	18	0.104	0.95			
	23	0.777	0.68			
	26	7.045	0.03	Trh-Gal4 (3) versus Trh > dTRPA1-mCherry	0.483	1.00
				UAS:dTRPA1-mCherry versus Trh > dTRPA1-mCherry	2.019	0.13
				UAS:dTRPA1-mCherry versus Trh-Gal4 (3)	2.502	0.04
	28	28.546	<0.0001	Trh-Gal4 (3) versus Trh > dTRPA1-mCherry	3.644	<0.001
				UAS:dTRPA1-mCherry versus Trh > dTRPA1-mCherry	5.206	<0.0001
				UAS:dTRPA1-mCherry versus Trh-Gal4 (3)	1.562	0.36
	30	56.769	<0.0001	Trh-Gal4 (3) versus Trh > dTRPA1-mCherry	7.248	<0.0001
				UAS:dTRPA1-mCherry versus Trh > dTRPA1-mCherry	5.402	<0.0001
				UAS:dTRPA1-mCherry versus Trh-Gal4 (3)	1.845	0.20
	32	52.443	<0.0001	Trh-Gal4 (3) versus Trh > dTRPA1-mCherry	6.513	<0.0001
				UAS:dTRPA1-mCherry versus Trh > dTRPA1-mCherry	5.998	<0.0001
				UAS:dTRPA1-mCherry versus Trh-Gal4 (3)	0.515	1.00

[a]Statistical comparisons (Kruskal–Wallis tests with multiple pairwise post hoc comparisons) for temperature-dependent decrease in locomotion velocity induced by dTRPA1-mCherry under control of the three Trh-Gal4 lines compared with the heterozygous Trh-Gal4 lines and the heterozygous UAS:dTRPA1-mCherry line, as shown in Figure 1E–G (n = 27 per group).

groups of 5-HT-positive neurons and, in addition, large numbers of 5-HT-negative neurons (Fig. 1C,D; Table 2), but cover different numbers of 5-HT-positive neurons. These differences could be determined by identifying soma clusters (Fig. 1C; Table 2). The nonspecific, 5-HT-negative neurons covered by these Gal4 lines are located in many diverse regions throughout the central brain, most prominent in the anterior protocerebrum, around the antennal lobes, in the pars intercerebralis, and in the posterior protocerebrum. However, to what degree these 5-HT-negative neurons potentially overlap between the three Trh-Gal4 lines could not be unambiguously determined. Using the thermosensitive cation channel, dTRPA1 (Hamada et al., 2008) under UAS control (Brand and Perrimon, 1993), we induced neuronal depolarization by raising the ambient temperature. dTRPA1 was fused with the red fluorescence protein, mCherry (Vasmer et al., 2014), to allow us to determine which neurons expressed the thermogenetic actuator construct (Fig. 1D). Raising the ambient temperature from 18°C to 32°C caused a gradual increase in locomotion activity in genetic control strains. However, when dTRPA1-mCherry was expressed under control of any of the three Trh-Gal4 strains, a drastic decrease in the animals' locomotion behavior was evident at temperatures between 28°C and 32°C (Fig. 1E–G). For exact statistical values, see Table 3.

In a second step, we tested whether this inhibition of locomotor behavior can be narrowed down to neurons in the brain. Of the three Gal4 lines, the Trh-Gal4 line (2) (Sitaraman et al., 2012), referred to as "Trh-Gal4" below, covered the greatest number of 5-HT-positive neurons and the smallest number of 5-HT-negative neurons when dTRPA1-mCherry was expressed (Fig. 1C,D; Table 2). This line was used for all further experiments. We restricted the expression of dTRPA1-mCherry to Trh-Gal4-positive brain neurons and excluded those located in the thoracic and abdominal ganglia using Tsh-Gal80 (Clyne and Miesenböck, 2008) (Fig. 2A). At 18°C locomotion velocity was not significantly different among the genotypes tested ($H_{(3, N = 109)}$ = 5.06, p = 0.17; Kruskal–Wallis test). However, significant differences were found at 32°C ($H_{(3, N = 108)}$ = 81.74, $p < 0.0001$; Kruskal–Wallis test) (Fig. 2B). Multiple pairwise *post hoc* comparisons revealed significant differences between animals expressing dTRPA1-mCherry under Trh-Gal4 control, either with Tsh-Gal80 or without Tsh-Gal80, and the heterozygous UAS: dTRPA1-mCherry; Tsh-Gal80 strain or the heterozygous Trh-Gal4 strain as controls ($p < 0.0001$ in all cases), but not between the two strains themselves (p = 1.0) (Fig. 2B). This shows that thermogenetically activating only these neurons located in the brain was sufficient to induce the decrease in locomotion activity
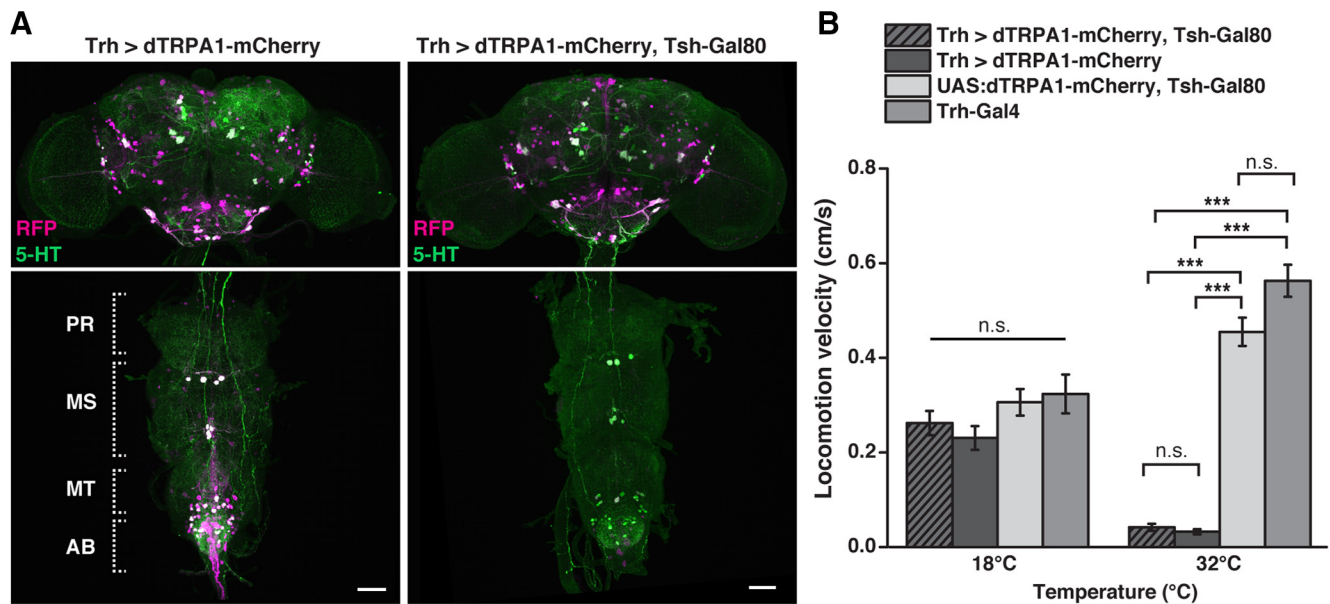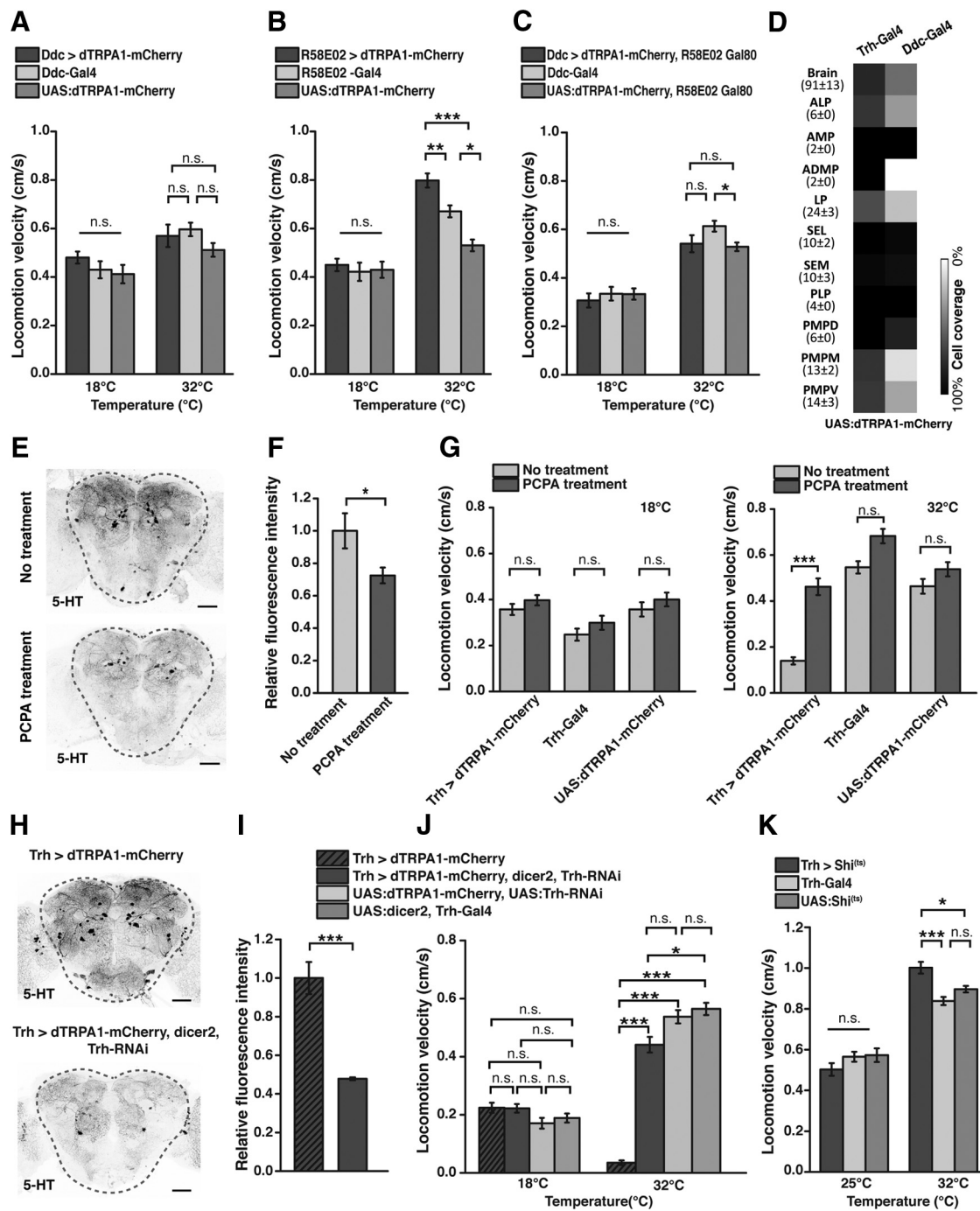
Figure 2. Behavioral quiescence is induced by 5-HT neurons in the brain. ***A***, Expression of dTRPA1-mCherry under control of Trh-Gal4 in the brain, the thoracic, and the abdominal ganglia (left). Gene expression is restricted to brain neurons using Tsh-Gal80 (right). Magenta represents anti-RFP immunoreactivity against dTRPA1-mCherry. Green represents anti-5-HT immunoreactivity. White represents the overlap. AB, Abdominal ganglia; MS, mesothoracic ganglia; MT, metathoracic ganglia; PR, prothoracic ganglia. Scale bars, 50 μm. ***B***, Thermogenetic activation of all Trh-Gal4-positive neurons and of Trh-Gal4-positive neurons in the brain only equally decreases locomotor activity. Bars indicate mean ± SEM ($n = 27$–28). n.s., Not significant ($p > 0.05$). ****p < 0.001$.

fully (Fig. 2*B*). Because the Ddc-Gal4 (Li et al., 2000) line also covers a large proportion of 5-HT neurons and, in addition, dopamine-releasing neurons of the PAM cluster (Pech et al., 2013), we tested whether thermogenetic activation of these neurons also results in an inhibition of locomotor activity. We found that thermogenetic activation of neurons covered by Ddc-Gal4 did not cause any change in locomotor activity (Fig. 3*A*). Neither at 18°C, nor at 32°C significant differences in locomotion velocity between Ddc > dTRPA1-mCherry and the heterozygous parental strains as controls were found (18°C: $H_{(2, N = 109)} = 1.645$, $p = 0.44$; 32°C: $H_{(2, N = 108)} = 6.079$, $p < 0.05$; Kruskal–Wallis test; pairwise *post hoc* comparisons between the three genotypes did not reveal significant differences ($p > 0.05$)). Ddc-Gal4 includes less 5-HT neurons than Trh-Gal4 (Fig. 3*D*), most obvious in the cell clusters ALP, ADMP, LP, PMPM, and PMPV, which suggests that not all 5-HT neurons, but only a fraction covered by Trh-Gal4 and not Ddc-Gal4, cause the decrease in behavioral activity. However, the release of DA has been implicated in arousal increase (Andretic et al., 2005; Kume et al., 2005), raising the alternative possibility that 5-HT and DA neurons compensate each other's behavioral effects. Indeed, activating dopaminergic neurons of the PAM-cluster using R58E02-Gal4 causes a significant increase in locomotion, although the two heterozygous parental strains also show significant differences at 32°C (Fig. 3*B*) (18°C: $H_{(2, N = 109)} = 1.50$, $p = 0.93$; 32°C: $H_{(2, N = 108)} = 35.89$, $p < 0.0001$; Kruskal–Wallis test; pairwise *post hoc* comparisons: R58E02 > dTRPA1-mCherry vs UAS:dTRPA1-mCherry: $p < 0.0001$; R58E02 > dTRPA1-mCherry vs R58E02-Gal4: $p < 0.01$; R58E02-Gal4 vs UAS:dTRPA1-mCherry: $p < 0.03$). To test for this possibility of compensatory effects, we excluded PAM cluster neurons from the cells covered by Ddc-Gal4 using R58E02-Gal80 (Liu et al., 2012a) and thereby restricted the dTRPA1-mCherry expression mainly to non-PAM-cluster neurons. Activating these neurons only again did not cause any change in locomotion (Fig. 3*C*), ruling out an effect of PAM cluster dopaminergic neurons counteracting a potential 5-HT-induced decrease in locomotion

activity (18°C: $H_{(2, N = 103)} = 0.48$, $p = 0.78$; 32°C: $H_{(2, N = 107)} = 7.22$, $p < 0.027$; Kruskal–Wallis test; pairwise *post hoc* comparisons between the three genotypes did not reveal significant differences between the strain Ddc > dTRPA1-mCherry, R58E02-Gal80, and the genetic control strains ($p > 0.13$)). These experiments suggest on the one hand that not all 5-HT neurons are equally involved in inducing a decrease in locomotor activity, but only those covered by Trh-Gal4, but not Ddc-Gal4. On the other hand, it confirms that the decrease in locomotor activity observed upon depolarization of Trh-Gal4-positive neurons is not a general phenomenon generated by the activation of aminergic neurons of any type.

Because Trh-Gal4 encompasses a large number of 5-HT-negative neurons (Fig. 1*D*; Table 2), we tested whether it is indeed 5-HT release that exerts an inhibitory effect on the animals' behavior. To this end, we fed the animals with para-chlorphenylalanine (PCPA), an inhibitor of tryptophan hydroxylase (Koe and Weissman, 1966) that has been shown to be effective in *Drosophila* (Dasari et al., 2007). 5-HT immunoreactivity was significantly decreased in animals treated with PCPA (Fig. 3*E*,*F*; $t_{(8)} = 2.3$, $p < 0.05$; Student's *t* test). Thermogenetically induced depolarization of Trh-Gal4-positive neurons in PCPA-treated animals showed a much less severe decrease in locomotion velocity (Fig. 3*G*). Although at 18°C significant differences in locomotion velocity among the three genotypes and pharmacological treatments tested were detected ($H_{(5, N = 211)} = 22.02$, $p < 0.0005$; Kruskal–Wallis test), pairwise *post hoc* comparisons between the flies with or without PCPA treatment did not reveal significant differences ($p > 0.85$ in all cases). However, at 32°C significant differences were detected across groups of animals ($H_{(5, N = 215)} = 95.22$, $p < 0.0001$; Kruskal–Wallis test), and pairwise *post hoc* comparisons revealed a significant difference between PCPA-treated and untreated animals of the genotype Trh > dTRPA1-mCherry ($p < 0.0001$), but not of the genotypes Trh-Gal4 ($p = 0.27$) and UAS:dTRPA1-mCherry ($p = 1.0$).

Figure 3. Behavioral quiescence is induced by serotonin. **A**, Thermogenetic activation of Ddc-Gal4-positive neurons does not induce any change in locomotor activity (*n* = 36 or 37). **B**, Thermogenetic activation of R58E02-Gal4-positive neurons induces higher locomotor activity (*n* = 35–37). **C**, Thermogenetic activation of Ddc-Gal4-positive neurons, but excluding dopaminergic neurons of the PAM cluster using R58E02-Gal80, does not induce any change in locomotor activity (*n* = 34–36). **D**, Coverage of 5-HT neurons by Ddc-Gal4 compared with Trh-Gal4. Numbers in parentheses indicate the total numbers of 5-HT-immunoreactive neurons for each cluster in both central brain hemispheres (mean ± SD, *n* = 18). Grayscale represents the relative coverage of these neurons by the two Gal4 lines when UAS:dTRPA1-mCherry is used as a reporter (*n* = 3 brains each). **E**, Feeding of PCPA reduces 5-HT immunoreactivity. Dashed lines indicate the region within the central brain used for quantification shown in **F**. Scale bar, 50 μm. **F**, PCPA partially reduces 5-HT levels (*n* = 5). **G**, The decrease in locomotion velocity induced by thermogenetic activation of Trh-Gal4-positive neurons is extenuated by PCPA feeding (*n* = 33–39). **H**, Downregulation of serotonin synthesis using Trh-RNAi leads to a reduction in 5-HT immunoreactivity. Dashed lines indicate the regions within the central brain used for quantification shown in **I**. Scale bar, 50 μm. **I**, Intensity of anti-5-HT immunoreactivity. Downregulation of tryptophan hydroxylase using Trh-RNAi reduces 5-HT levels (*n* = 4). **J**, The decrease in locomotion velocity induced by thermogenetic activation of Trh-Gal4-positive neurons is extenuated by Trh-RNAi expression (*n* = 37–45). **K**, Blocking synaptic transmitter release from Trh-Gal4-positive neurons using UAS:shi$^{(ts)}$ causes an increase in locomotor activity (*n* = 35–41). Bars indicate mean ± SEM. n.s., Not significant (*p* > 0.05). *p < 0.05. **p < 0.01. ***p < 0.001.

As a second test, we knocked down tryptophan hydroxylase using Trh-RNAi, which significantly decreased 5-HT immunoreactivity ($t_{(6)}$ = 6.3, *p* < 0.001; Student's *t* test; Fig. 3 *H,I*). Again, locomotion activity was to a large degree restored in these ani-

mals during thermogenetic activation of Trh-Gal4-positive neurons (Fig. 3*J*). Whereas at 18°C no difference between the four genotypes tested was detected ($H_{(3, N = 159)}$ = 8.31, *p* < 0.04; Kruskal–Wallis test; pairwise *post hoc* comparisons: *p* > 0.09 in all
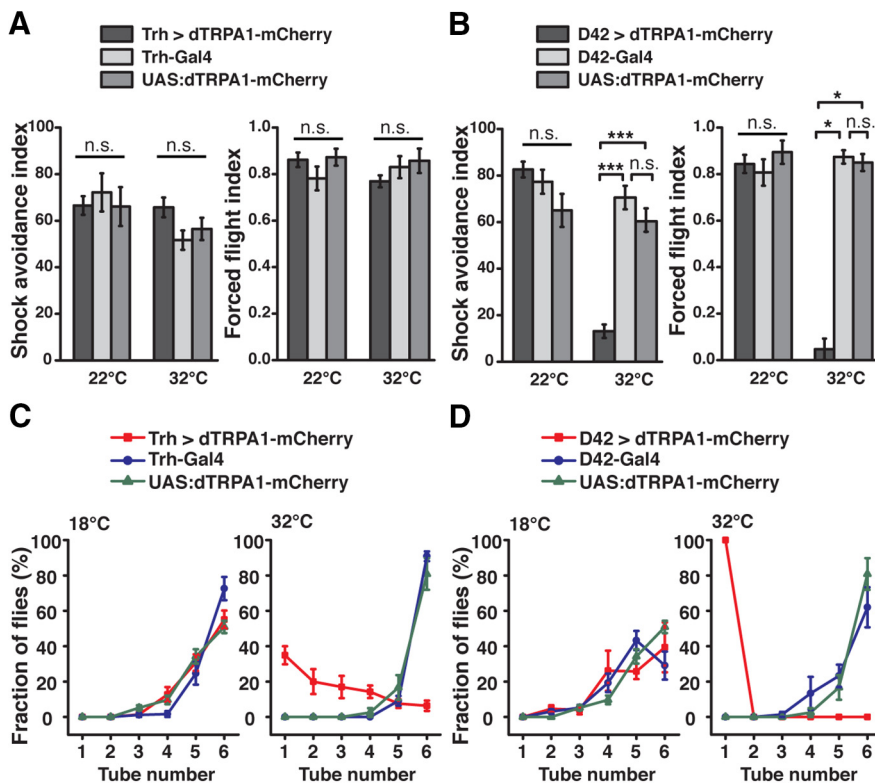
Figure 4. Thermogenetic activation of 5-HT neurons does not affect locomotor abilities. **A**, Electric shock avoidance (left panel, n = 10 or 11) and forced flight (right panel, n = 5) are unaffected in flies expressing dTRPA1-mCherry under control of Trh-Gal4, both at 22°C and 32°C, compared with the heterozygous parental strains. **B**, In flies expressing dTRPA1-mCherry in motor neurons under control of D42-Gal4, thermogenetic neuronal activation impairs electric shock avoidance (left panel, n = 10 or 11) and forced flight (right panel, n = 5) at the effective temperature of 32°C, but not at 22°C. **C**, Negative geotaxis behavior assayed by countercurrent distribution at 18°C (left) and 32°C (right) in flies expressing dTRPA1-mCherry under control of Trh-Gal4 compared with the heterozygous parental strains. At 18°C, no difference between the strains is observed. At 32°C, negative geotaxis is attenuated, but not abolished, in flies expressing dTRPA1-mCherry under control of Trh-Gal4 (n = 5). **D**, Negative geotaxis behavior of flies expressing dTRPA1-mCherry under control of D42-Gal4 is indistinguishable from the heterozygous parental lines at 18°C (left). At 32°C (right), negative geotaxis is completely abolished in flies expressing dTRPA1-mCherry under control of D42-Gal4 (n = 5). Data points and bars indicate mean ± SEM. n.s., Not significant (p > 0.05). *p < 0.05. ***p < 0.001.

cases), at 32°C a significant difference among genotypes was detected ($H_{(3, N = 108)}$ = 93.88, $p < 0.0001$; Kruskal–Wallis test), and in pairwise *post hoc* comparisons the severely decreased locomotion velocity in flies of the genotype Trh > dTRPA1-mCherry was significantly different from those animals expressing in addition the Trh-RNAi construct along with dicer2 ($p > 0.0001$). These results confirm that it is indeed 5-HT-release that underlies the thermogenetically induced behavioral hypoactivity.

To test further whether blocking transmitter release from Trh-Gal4-positive neurons caused the opposite behavioral effect, we expressed temperature-sensitive shibire[(ts)] (Kitamoto, 2001; Pfeiffer et al., 2012) under control of this driver line. At the restrictive temperature of 32°C the overall activity of the genetic control strains was already higher compared with the permissive temperature the animals had been raised at (25°C). However, on top of that increased behavioral activity, blocking synaptic transmission from Trh-Gal4-positive neurons further increased the animals' locomotion velocity significantly (Fig. 3K) (25°C: $H_{(2, N = 110)}$ = 2.16, $p = 0.34$; 32°C: $H_{(2, N = 113)}$ = 21.19, $p < 0.0001$; Kruskal–Wallis test). Pairwise *post hoc* comparisons between the three genotypes revealed significant differences between the strain Trh > shi[(ts)] and Trh-Gal4 ($p < 0.0001$), and UAS:shi[(ts)] ($p < 0.02$), but not between Trh-Gal4 and UAS:shi[(ts)] ($p = 0.25$).

Thermogenetic activation of 5-HT-releasing neurons does not affect motor abilities but induces behavioral quiescence

Next, we asked whether this behavioral hypoactivity was a result of a mere locomotion deficit. Therefore, we subjected the animals to an avoidance assay in which they were forced to escape electric shocks. Thermogenetic activation of Trh-Gal4-positive neurons did not affect their performance at all compared with genetic control animals (22°C: $H_{(2, N = 32)}$ = 1.25, $p = 0.54$; 32°C: $H_{(2, N = 31)}$ = 4.54, $p = 0.1$; Kruskal–Wallis test; Fig. 4A). Likewise, in a forced flight assay, activation of 5-HT-releasing neurons did not impair the animals' ability to fly when agitated (22°C: $H_{(2, N = 15)}$ = 1.52, $p = 0.47$; 32°C: $H_{(2, N = 15)}$ = 2.66, $p = 0.26$; Kruskal–Wallis test; Fig. 4A). As a positive control for the assay, we activated a large proportion of brain and thoracic neurons thermogenetically, including motor neurons, using D42-Gal4 (Parkes et al., 1998), which resulted in a drastic inability of the flies to escape electric shocks (22°C: $H_{(2, N = 30)}$ = 3.66, $p = 0.16$; 32°C: $H_{(2, N = 30)}$ = 20.11; $p < 0.0001$; Kruskal–Wallis test; pairwise *post hoc* comparisons between D42 > dTRPA1-mCherry and genetic control strains: $p < 0.0001$ in all cases; Fig. 4B) and, likewise, in an almost complete impairment in their flight ability (22°C: $H_{(2, N = 15)}$ = 1.24, $p = 0.54$; 32°C: $H_{(2, N = 15)}$, $p < 0.01$; Kruskal–Wallis test; *post hoc* comparisons between D42 > dTRPA1-mCherry and genetic control strains: $p < 0.04$ in all cases) (Fig. 4B).

The finding that activating 5-HT-releasing neurons affects the animals' overall behavioral activity, but leaves motor abilities intact, is already apparent when simply observing the behavior of animals kept in vials. Tapping the flies down to the bottom of the vials initiates a negative geotaxis response (Benzer et al., 1967). However, under conditions of thermogenetic activation of Trh-Gal4-positive neurons, the flies' overall activity declined shortly after this startle-induced climbing response. We quantified this behavioral effect in a negative geotaxis assay (Inagaki et al., 2010). When Trh-Gal4-positive neurons were thermogenetically depolarized, the animals showed delayed, but not completely abolished, negative geotaxis (Fig. 4C). In contrast, when motor neurons were depolarized using D42-Gal4, no negative geotaxis behavior was observed at all (Fig. 4D). These data confirm again that, when 5-HT release is induced, the animals are able to move. They just do not unless they are startled by a stimulus, a phenomenon we refer to as behavioral quiescence.

Thermogenetic activation of 5-HT-releasing neurons reduces motivational behavior

The modulation of endogenous behavior by intrinsic factors or "states" represents a typical feature of motivational behavior. Therefore, we tested whether activating 5-HT-releasing neurons affects complex, motivation-driven behavior. Sex-related drive
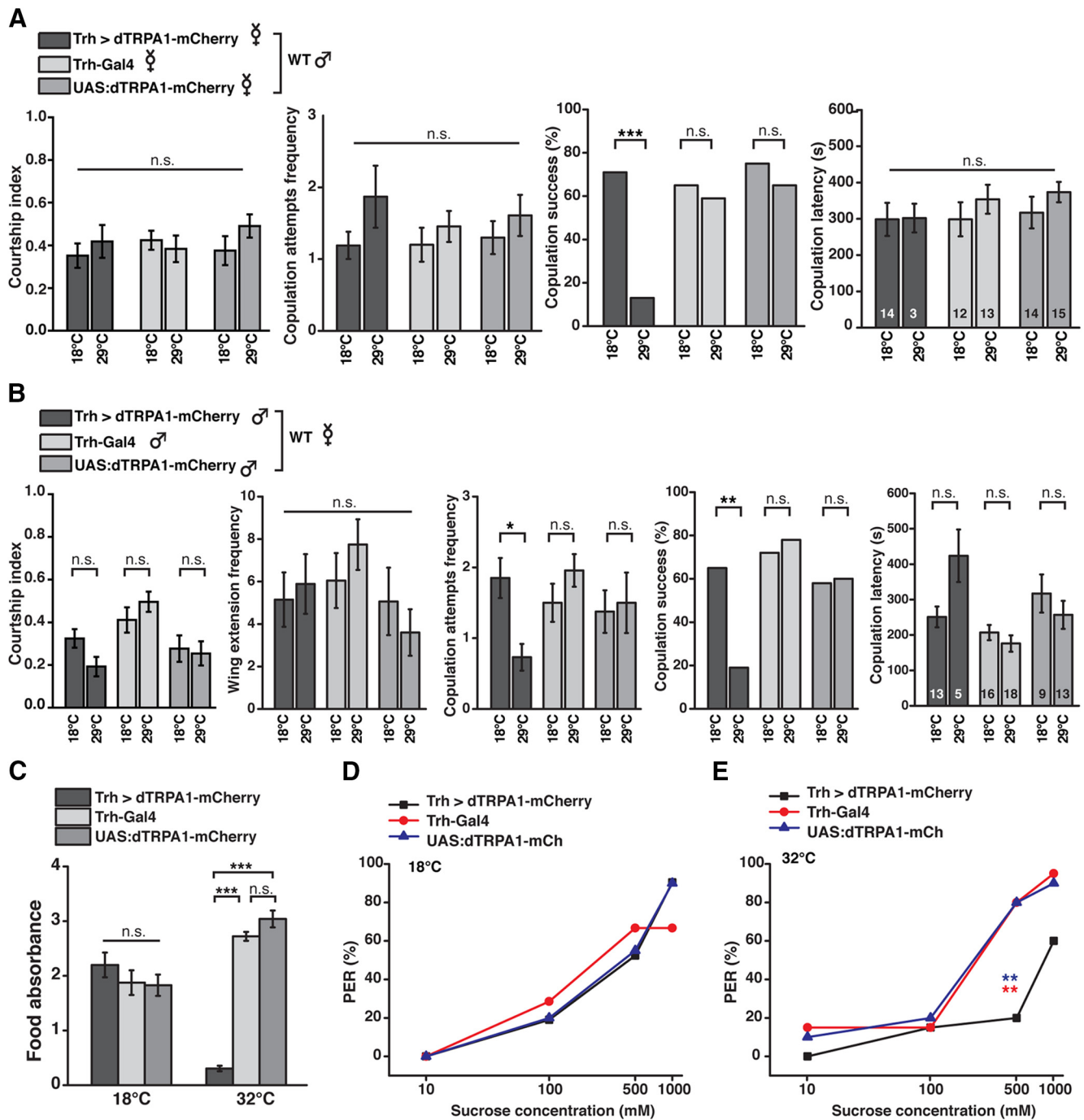
Figure 5. 5-HT neurons reduce motivated behaviors and sensory responsiveness. *A*, Mating behavior of wild-type males toward virgin females expressing dTRPA1-mCherry under Trh-Gal4 control or toward genetic control strains was quantified at 18°C and 29°C. For neither female genotype, male courtship index, frequency of male copulation attempts, or copulation latency of those males that succeeded to copulate (*n* indicated within the bars) was significantly different between 18°C and 29°C. Copulation success (female receptivity) was significantly reduced due to thermogenetic activation of Trh-Gal4-positive neurons. *n* = 20 –23. *B*, Mating behavior of males expressing dTRPA1-mCherry under Trh-Gal4 control or of genetic control strains toward wild-type virgin females was quantified at 18°C and 29°C. Thermogenetic activation of Trh-Gal4-positive neurons in males did not significantly reduce courtship index or wing extension frequency, but copulation attempts frequency and copulation success (*n* = 16 –23). Those males that succeeded to copulate showed no statistically significant difference at the given sample size (*n* indicated within the bars). *C*, Food uptake is significantly reduced in starved flies expressing dTRPA1-mCherry under control of Trh-Gal4 at 32°C, but not at 18°C (*n* = 5). *D*, *E*, Sucrose-induced proboscis extension reflex (PER) was quantified at 18°C (*D*) and 32°C (*E*) in flies expressing dTRPA1-mCherry under control of Trh-Gal4 and in genetic control strains. Thermoactivation of 5-HT neurons shifts gustatory responsiveness toward higher sucrose concentrations (*n* = 20 or 21). Bars and data points indicate means; error bars indicate SEM. n.s., Not significant (*p* > 0.05). *p < 0.05. **p < 0.01. ***p < 0.001.

represents a motivational factor influencing mating behavior. We find that the overall courtship index, comprising several aspects of courtship and mating behavior, of sexually deprived wild-type males toward virgin females in which 5-HT neurons were depolarized was indistinguishable from their behavior toward females

of genetic control strains or between ambient temperatures ($H_{(5, N = 129)}$ = 3.77, *p* = 0.58; Kruskal–Wallis test; Fig. 5A). Likewise, the number of copulation attempts ($H_{(5, N = 120)}$ = 1.92, *p* = 0.87; Kruskal–Wallis test) and copulation latency ($H_{(5, N = 120)}$ = 2.90, *p* = 0.72; Kruskal–Wallis test) was not significantly affected
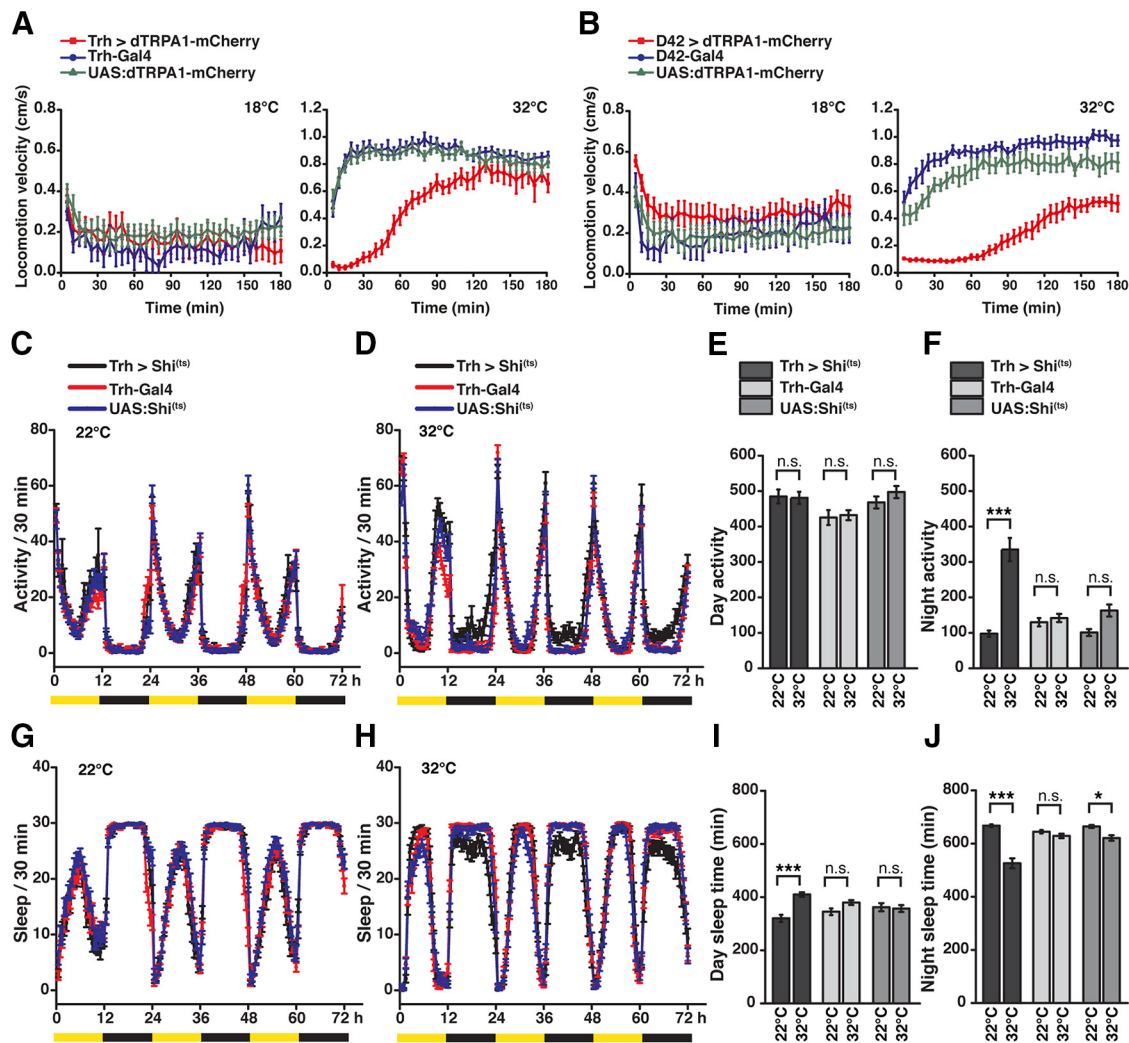
Figure 6. Blocking synaptic output from 5-HT neurons affects circadian activity and sleep. **A**, The locomotion velocity of the flies expressing dTRPA1-mCherry under Trh-Gal4 control and the heterozygous parental lines were monitored for 3 h at 18°C and 32°C. Locomotion velocity over a 3 h time course was indistinguishable among all groups at 18°C. At 32°C, initial locomotion velocity of flies expressing dTRPA1-mCherry under Trh-Gal4 control was reduced compared with the parental controls. However, after ∼45 min, the Trh > dTRPA1-mCherry flies recovered from quiescence and locomotion velocity returned to baseline after ∼120 min. **B**, The locomotion velocity of the flies expressing dTRPA1-mCherry under D42-Gal4 control and the heterozygous parental lines were monitored for 3 h at 18°C and 32°C. Locomotion velocity over a 3 h course time was indistinguishable among all groups at 18°C. At 32°C, flies expressing dTRPA1-mCherry under D42-Gal4 control paralyzed. However, after ∼70 min, the D42 > dTRPA1-mCherry flies recovered from paralysis and locomotion increased. Dots indicate mean ± SEM for 5 min time bins (*n* = 8 or 9). **C–F**, Circadian locomotion activity over 72 h at light-dark cycles indicated by yellow/black bars compared between flies expressing shi[(ts)] under control of Trh-Gal4 and genetic controls at the permissive temperature of 22°C (**C**) and the restrictive temperature of 32°C (**D**). Quantification of total day (**E**) and night activity (**F**) at 22°C and 32°C. **G–J**, Sleep time per 30 min during 72 h, indicated by yellow/black bars (mean ± SEM), at the permissive temperature of 22°C (**G**) and the restrictive temperature of 32°C (**H**). Quantification of total sleep time during day time (**I**) and night time (**J**). *n* = 42 or 43. Data points in line diagrams indicate mean ± SEM in 30 min time bins; bars indicate means ± SEM. n.s., Not significant (*p* > 0.05). **p < 0.05. ***p < 0.001.

by activating the females' 5-HT neurons. However, their copulation success was drastically reduced at 29°C compared with 18°C (Trh > dTRPA1-mCherry: *p* < 0.0005; Trh-Gal4: *p* = 0.76; UAS: dTRPA1-mCherry: *p* = 0.52; Fisher's exact test; Fig. 5A). Interestingly, the wild-type males' failure in mating was due to the females' active behavior: Those virgins whose 5-HT-releasing neurons were depolarized actively prevented the males from copulating by engaging in evasive movements. Males whose 5-HT-releasing neurons were thermogenetically depolarized showed no significantly reduced overall courtship activity at 29°C compared with 18°C (H$_{(5, N = 127)}$ = 23.23, *p* < 0.001; Kruskal–Wallis test; pairwise *post hoc* comparisons between temperatures: *p* > 0.65 for each genotype), and, as one aspect of courtship behavior, no reduced wing extension frequency (H$_{(5, N = 127)}$ = 9.34, *p* = 0.1; Kruskal–Wallis test). However, they showed significantly less

copulation attempts (H$_{(5, N = 127)}$ = 16.12, *p* < 0.007; Kruskal–Wallis test; *post hoc* comparisons between 18°C and 29°C in Trh > dTRPA1-mCherry: *p* < 0.04, and between 18°C and 29°C in Trh-Gal4 or UAS:dTRPA1-mCherry: *p* = 1.0 each) and, consequently, had significantly lower success in copulating (Trh > dTRPA1-mCherry: *p* < 0.01; Trh-Gal4: *p* = 0.74; UAS:dTRPA1-mCherry: *p* = 1.0; Fisher's exact test). And those few animals that were successful in copulating showed an increased latency to copulation by trend, although this was not statistically significant, most likely due to the low sample size of males showing copulation behavior (H$_{(5, N = 74)}$ = 15.50, *p* < 0.008; Kruskal–Wallis test; pairwise *post hoc* comparisons did not reveal significant differences between 18°C and 29°C in all three genotypes (*p* = 1.0 each); Fig. 5B). In summary, activating 5-HT neurons negatively affects the animals' mating behavior by inhibiting both female
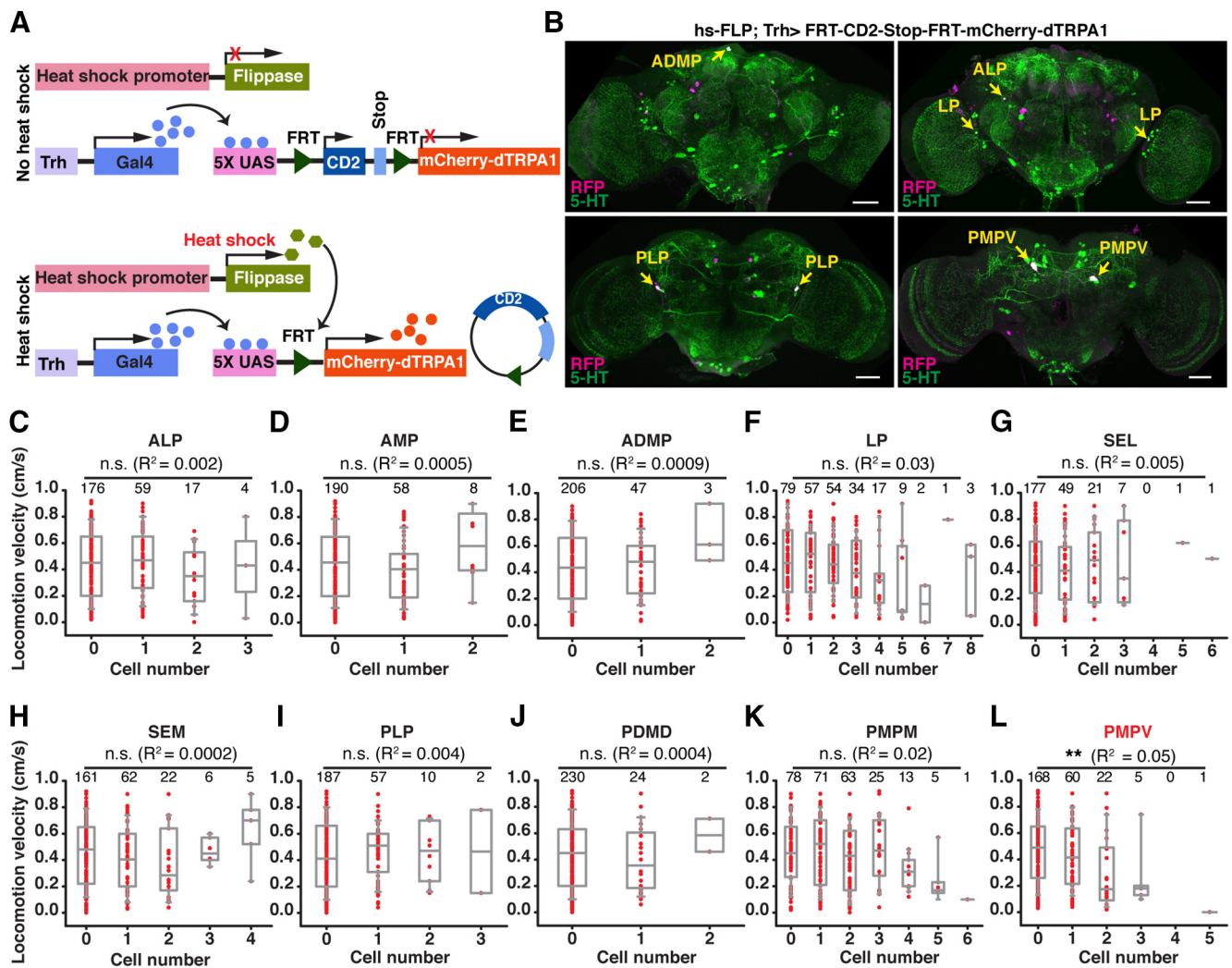
Figure 7. Stochastic activation of subsets of 5-HT neurons indicates a role of PMPV neurons for inducing behavioral quiescence. ***A***, Schematic illustration of stochastically expressing mCherry-dTRPA1 in random subsets of Trh-Gal4-positive neurons using a UAS:FRT-CD2-stop-FRT-mCherry-dTRPA1 line and a flippase (FLP) under heat-shock promoter control. ***B***, Representative examples for stochastic expression of mCherry-dTRPA1 in subsets of 5-HT neurons. Magenta represents anti-RFP immunoreactivity against mCherry-dTRPA1. Green represents anti-5-HT immunoreactivity. White represents the overlap. Yellow arrows indicate 5-HT neurons expressing mCherry-dTRPA1. Scale bars, 50 μm. ***C–L***, Effect of the number of activated 5-HT neurons in specific clusters on locomotion velocity. The dataset for each panel is obtained from 256 flies expressing mCherry-dTRPA1 stochastically in different subsets of neurons. The cluster names are indicated above the respective panels. Red dots indicate the locomotion velocity for individual flies expressing mCherry-dTRPA1 in the indicated number of neurons. Box plots (gray) represent medians and interquartile ranges. Whiskers represent 10/90 percentiles for each group of flies with distinct numbers of thermoactivated 5-HT neurons in a defined cluster. Regression analysis (R^2 values indicated) revealed only for the PMPV cluster (***L***) a significant difference in locomotion velocity among flies expressing mCherry-dTRPA1 in different numbers of neurons. No significant difference was observed for all other neuron clusters. n.s., Not significant ($p > 0.05$). **$p < 0.01$.

receptivity and male copulation behavior, but leaves aspects of male courtship (e.g., wing extension behavior) intact.

Hunger or appetite represents a motivational factor driving feeding behavior. Therefore, as a second type of motivation-driven behavior, we quantified the animals' food uptake. Animals were motivated to feed by 48 h of starvation, were subsequently placed on sweet food containing a red dye, and were allowed to feed for 45 min. Spectrophotometric quantification of red dye absorbance revealed that those animals whose Trh-Gal4-positive neurons were thermogenetically depolarized during the feeding period consumed drastically less food than the respective genetic control strains (18°C: $F_{(2,12)} = 0.87$, $p = 0.44$; 32°C: $F_{(2,12)} = 202.71$, $p < 0.001$; one-way ANOVA; pairwise *post hoc* Bonferroni tests detected a significant difference between flies expressing dTRPA1-mCherry and the respective control strains ($p < 0.001$), but not between the UAS and the Gal4 strain ($p = 0.16$); Fig. 5C). This demonstrates that food uptake behavior is also

negatively affected by the release of 5-HT. Because feeding behavior is affected by the artificial activation of Trh-Gal4-positive neurons, we tested the animals' responsiveness to gustatory sugar stimuli of varying intensities by observing proboscis extension. Those animals that expressed dTRPA1-mCherry under control of Trh-Gal4 showed an increased response threshold shifted to higher sucrose concentrations, with a significantly reduced response at 500 mM sucrose at 32°C ($p < 0.002$; Fisher's exact test with Bonferroni correction), but not at 18°C ($p > 0.39$ at all sucrose concentrations and between genotype comparisons; Fisher's exact test with Bonferroni correction; Fig. 5D,E). This could reflect either a direct, peripheral reduction in sensory responsiveness and/or an influence on more central, appetite/hunger-mediating circuits. In conclusion, at least two complex types of behavior influenced by motivational factors (i.e., appetite/hunger and reproductive motivation, respectively) are inhibited by depolarizing 5-HT neurons.

A

B

actin-FRT-Stop-FRT-Gal4; UAS:GFP, Trh-FIF II   actin-FRT-Stop-FRT-Gal4; UAS:GFP; Trh-FIF III
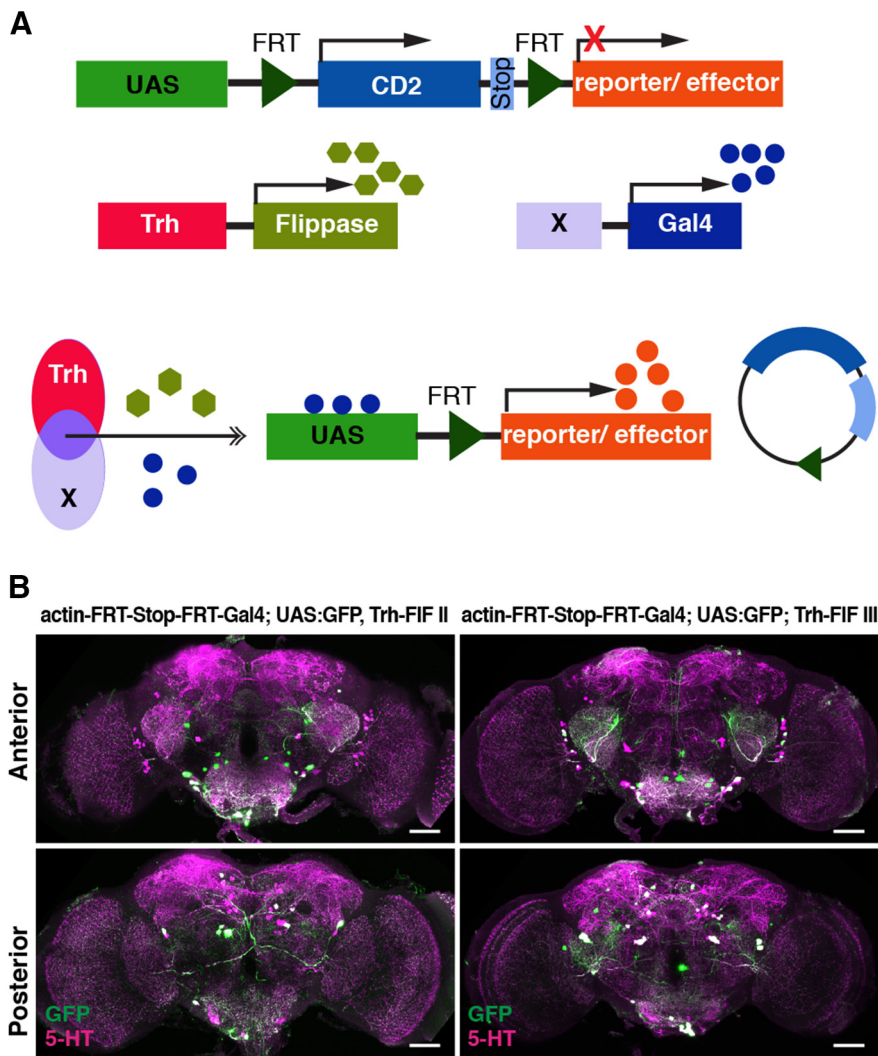
Figure 8. Restriction of gene expression to 5-HT neurons using flippase under control of a Trh promoter sequence. *A*, Schematic illustration of the intersectional gene expression of transgenes in defined subsets of 5-HT neurons using UAS:FRT-CD2-stop-FRT-reporter/effector, Trh-flippase, and diverse (X) Gal4 lines. *B*, Immunohistochemical stainings of brains are shown across stacks of confocal images as z-axis projections of maximal fluorescence intensity from anterior (top row) or posterior view (bottom row). GFP expression (green) is driven in those neurons in which a stop codon is removed through flippase (FIF) expression under control of a Trh promoter. Magenta represents anti-5-HT immunoreactivity. Left side represents Trh-FIF insertion on the second chromosome. Right side represents Trh-FIF insertion on the third chromosome. GFP expression is driven predominantly in a large proportion of 5-HT-positive neurons. Scale bars, 50 μm.

Gal4-positive neurons using shibire$^{(ts)}$ over 3 d at 12 h:12 h light-dark conditions. At both the permissive temperature of 22°C and the restrictive temperature of 32°C, the animals showed normal circadian rhythms (Fig. 6C,D). Blocking synaptic transmission from 5-HT neurons did not affect the flies' overall activity during day ($H_{(5, N = 252)} = 16.98$, $p < 0.005$; Kruskal–Wallis test; *post hoc* comparisons between the temperatures within each genotype did not detect statistical significance ($p = 1.0$ in all cases); Fig. 6E). However, a drastic increase in activity was observed during night ($H_{(5, N = 252)} = 63.89$; $p < 0.0001$; Kruskal–Wallis test; *post hoc* comparisons between the temperatures for each genotype revealed statistical significance for Trh > Shi$^{(ts)}$ ($p < 0.0001$), but not the control strains Trh-Gal4 ($p = 1.0$) or UAS:Shi$^{(ts)}$ ($p = 0.12$); Fig. 6F).

When the animals' overall sleep time, which is in contrast to the animals' mere activity defined as continuous 5 min periods of inactivity (Shaw et al., 2000), was counted (Fig. 6G,H), we observed increased sleep during the day ($H_{(5, N = 252)} = 30.16$, $p < 0.0001$; Kruskal–Wallis test; *post hoc* comparisons revealed statistical significance for Trh > Shi$^{(ts)}$ ($p < 0.0001$), but not the control strains Trh-Gal4 ($p = 0.78$) or UAS:Shi$^{(ts)}$ ($p = 1.0$); Fig. 6I). During the night, the opposite effect was observed ($H_{(5, N = 252)} = 72.96$; $p < 0.0001$; Kruskal–Wallis test; *post hoc* comparisons revealed statistical significance for Trh > Shi$^{(ts)}$ ($p < 0.0001$), a slight difference for UAS:Shi$^{(ts)}$ ($p = 0.014$), but not for Trh-Gal4 ($p = 1.0$) i.e., a decrease in sleep; Fig. 6J), in accordance with the increase in overall locomotor activity (Fig. 6F). The oppositional effects of blocking 5-HT release during day and night might point toward the possibility that the animals during daytime compensate for sleep loss caused by the higher activity during night. The finding that blocking transmission from Trh-positive neurons leads to increased daytime sleep, but leaves the overall daytime locomotion activity unaffected, reflects the different parameters (activity vs sleep) tested: These animals show less fragmented and less interrupted locomotor activity, detected as more periods of continuous (>5 min) inactivity, which constitutes the defining criterion for sleep in flies.

Stochastic dissection of the serotoninergic neuronal circuitry
We sought next to determine whether the induction of behavioral quiescence, observed as decreased endogenously generated locomotion, was caused by an overall, neurohumoral release of 5-HT floating in large parts of the fly's brain, or whether distinct and localized neurons mediate this function. To restrict the analysis to a smaller number of candidate neurons, we first conceived a stochastic gene expression approach (Fig. 7A). We used trans-
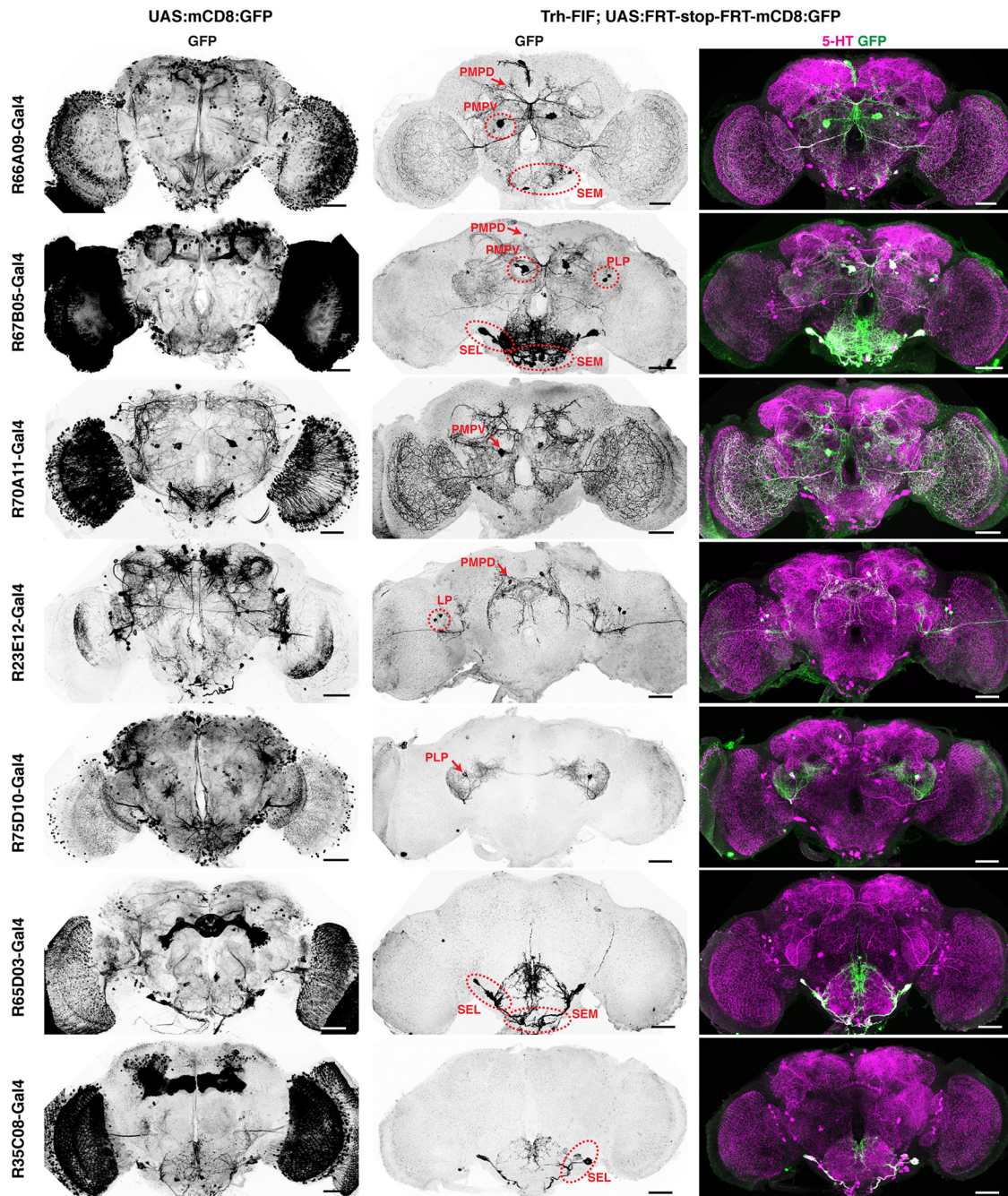
Because an animals' activity state is closely associated with circadian sleep–wake cycles (Brown et al., 2012), and 5-HT has been suggested as a sleep-promoting factor in *Drosophila* (Yuan et al., 2006; Nall and Sehgal, 2014), we also tested whether manipulating Trh-Gal4-positive neurons affects sleep. However, activating neurons using dTRPA1-mCherry in long-term experiments over several days is not feasible: The thermogenetically induced behavioral inactivity upon depolarization of Trh-Gal4-positive releasing neurons slowly ceases after ~45 min and vanishes almost completely after ~120 min (Fig. 6A). This transient effect of dTRPA1-mCherry-mediated neuronal activation is not restricted to Trh-Gal4-positive neurons; a similar effect can be seen upon stimulation of motor neurons using D42-Gal4 (Fig. 6B), which might reflect either potential desensitization of dTRPA1 or neuronal adaptation to prolonged depolarization at the cellular or circuit level (Bianchi et al., 2012). Therefore, we used the converse approach and blocked synaptic transmission from Trh-

Figure 9.   Restriction of gene expression to confined 5-HT neurons using intersectional genetics. Expression of mCD8:GFP (anti-GFP immunoreactivity) in the brain under control of different Gal4 driver lines using the UAS-Gal4 system (left column) and restriction of mCD8:GFP expression to defined 5-HT neurons (middle and right columns). Middle column represents anti-GFP immunostainings. Right column represents the overlap of anti-GFP staining (green) and anti-5-HT immunoreactivity (magenta). The identities and positions of 5-HT neuron clusters expressing mCD8:GFP are indicated by red arrows and dashed circles. Scale bars, 50 μm.

genic flies that expressed mCherry-dTRPA1 downstream of a stop cassette flanked by two flippase recognition target (FRT) sequences (Vasmer et al., 2014). Flies that carried this DNA construct together with a flippase construct under control of a heat shock promoter (Basler and Struhl, 1994) express mCherry-dTRPA1 in random subpopulations of neurons under Gal4 control (Vasmer et al., 2014). In combination with the Trh-Gal4 driver line, we obtained mosaic flies that expressed mCherry-dTRPA1 in random subsets of Trh-Gal4-positive neurons (Fig. 7B, representative examples). Only those neurons that expressed dTRPA1 were amenable to selective, thermogenetically induced

membrane depolarization. We determined the intrinsically generated locomotion velocity of 256 animals at 32°C and subsequently determined immunohistochemically the expression of mCherry-dTRPA1 in the brain. Using coimmunostaining against 5-HT, the mCherry-dTRPA1-expressing neurons could be unambiguously assigned to distinct neuronal somata clusters (Fig. 7B). By comparing the individual flies' locomotion velocity with the number of neurons activated for each 5-HT cell cluster, we found that increasing numbers of 5-HT neurons excited in the majority of neuronal clusters (ALP, AMP, ADMP, LP, SEL, SEM, PLP, PMPD, PMPM) did not significantly alter the mean

Table 4. Quantification of 5-HT and non-5-HT neurons expressing flippase under control of a Trh promoter[a]

| 5-HT clusters	Trh-FIF (II), FLP reporter	Trh-FIF (III), FLP reporter
ALP	1 ± 1	0 ± 0
AMP	1 ± 1	0 ± 0
ADMP	0 ± 0	0 ± 0
LP	8 ± 4	7 ± 2
SEL	7 ± 3	7 ± 4
SEM	5 ± 0	5 ± 1
PLP	3 ± 1	4 ± 0
PMPD	3 ± 1	4 ± 2
PMPM	2 ± 0	2 ± 1
PMPV	5 ± 1	9 ± 1
∑ 5-HT neurons	33 ± 1	36 ± 7
Non-5-HT neurons	11 ± 1	8 ± 1

[a]The numbers of 5-HT-positive and 5-HT-negative neurons expressing FIF and their soma cluster designation were immunohistochemically characterized in animals carrying DNA constructs for actin-FRT-Stop-FRT-Gal4, UAS:GFP, and either Trh-FIF located on the second chromosome (II) or third chromosome (III). Anti-GFP immunostaining was used to report flippase activity in combination with anti-5-HT immunostaining. Numbers indicate mean ± SD (n = 3 entire brains).

locomotion activity (Fig. 7C–K). There was no significant correlation between the number of somata expressing mCherry-dTRPA1 and the animals' locomotion velocity ($p > 0.08$; multiple regression analysis with *post hoc* Bonferroni correction). This indicates that behavioral quiescence is induced by 5-HT release from specific types of 5-HT neurons. However, the number of neurons thermogenetically activated within the PMPV cluster had a significant impact on the animals' locomotion activity (Fig. 7L; $p < 0.004$; multiple regression analysis with *post hoc* Bonferroni correction). Depolarizing neurons within this cell cluster decreased the flies' activity level, and hypoactivity increased as the number of activated neurons increased. This indicated a potential function of PMPV cluster neurons in inducing behavioral quiescence and led us to analyze these neurons in detail.

Thermogenetic activation of distinct 5-HT-releasing neurons of the PMPV cluster induces behavioral quiescence
To specifically manipulate neurons of the PMPV cluster only, we developed an intersectional gene expression strategy (Fig. 8A). First, we screened expression patterns of a large collection of Gal4 driver lines (Jenett et al., 2012) for expression in PMPV neurons, and selected 30 Gal4 lines that drove gene expression in at least one 5-HT-positive neuron, in addition to various numbers of diverse 5-HT-negative cells. Seven Gal4 lines were selected that showed UAS-controlled expression of the marker, mCD8-GFP, in few 5-HT-immunoreactive neurons (Fig. 9, left column), and we genetically combined them with the insertion of mCherry-dTRPA1 downstream of a FRT-flanked stop cassette (Vasmer et al., 2014). To restrict the mCherry-dTRPA1 expression to 5-HT-positive neurons, we generated transgenic fly lines expressing two copies of flippase interlinked by an IRES sequence (FIF) (Bohm et al., 2010) under direct control of the Trh promoter (Alekseyenko et al., 2010). We confirmed the functionality of two Trh-FIF lines by crossing them with a transgenic line carrying both actin-FRT-Stop-FRT-Gal4 and UAS-GFP (Pignoni and Zipursky, 1997) (Fig. 8B; Table 4). Using Trh-FIF, we restricted transgene expression with the selected Gal4 lines to 5-HT-positive neurons only (Fig. 9, middle and right columns). Three Gal4 lines (R66A09-Gal4, R67B05-Gal4, and R70A11-Gal4) included subsets of PMPV cluster neurons. The overall ~7 neurons per hemisphere within this cluster (Fig. 1A,B; Table 2) include one conspicuous neuron with a large soma and very widespread neurite arboriza-

tion in the optic lobes and large parts of the protocerebrum. This neuron is covered by all three Gal4 lines (Fig. 9). The remaining 5-HT-positive neurons of the PMPV cluster are characterized by smaller somata. Two pairs of these neurons are included in both R66A09-Gal4 and R67B05-Gal4 (Fig. 9). Because R66A09-Gal4 and R67B05-Gal4 also show expression within the PMPD, PLP, SEM and SEL. We added to our analysis four additional Gal4 lines (R23E12-Gal4, R75D10-Gal4, R65D03-Gal4, and R35C08-Gal4) that cover neurons in these clusters, respectively (Fig. 9). As expression levels can depend on the particular UAS line and the reporter used (Thum et al., 2006), we confirmed that these expression patterns are comparable when expressing mCherry-dTRPA1 (Fig. 10A). Overall, the intersectional strategy allows for a very selective, thermogenetic depolarization of distinct 5-HT neurons. When tested for locomotion velocity, no significant differences at 18°C between the flies expressing mCherry-dTRPA1 and the respective Gal4 strains or the UAS strain were observed ($H_{(14, N = 438)} = 46.67$, $p < 0.001$; Kruskal–Wallis test; pairwise *post hoc* comparisons: $p = 1.0$ in all cases; Fig. 10B). However, at 32°C, depolarization of neurons covered by R66A09-Gal4 or R67B05-Gal4 caused a significant decrease in locomotion velocity compared with the respective control strains ($H_{(14, N = 464)} = 130.73$, $p < 0.001$; Kruskal–Wallis test; pairwise *post hoc* comparisons: $p < 0.001$ for both strains; Fig. 10C). Nevertheless, the sedative effect on the flies using R66A09-Gal4 or R67B05-Gal4 was not as intense as that observed using Trh-Gal4 (Fig. 1E–G). Because both Gal4 lines encompass the pair of PMPV neurons with the large somata and, in addition, two pairs of PMPV neurons with smaller somata, we sought to identify those neurons that cause behavioral quiescence. Therefore, we tested the R70A11-Gal4 line that could be used to restrict mCherry-dTRPA1 solely to the pair of large neurons. Activation of the large PMPV neurons alone did not alter locomotion velocity at all ($p = 1.0$; Fig. 10C), which narrowed down the behavioral, quiescence-inducing effect to the small neurons within the PMPV cluster. In addition, we could rule out a sedative effect of depolarizing PMPD, SEM, SEL and PLP neurons (which are included in R66A09-Gal4 or R67B05-Gal4 driven expression) as using Gal4 lines that induce expression in these clusters, but not in the PMPV cluster, did not cause any change in locomotor velocity ($p = 1.0$; Fig. 10C). This combinatorial evaluation (Table 5) suggests that the activity of two pairs of 5-HT neurons located in the PMPV cluster is sufficient to induce behavioral quiescence. Of course, the possibility that more 5-HT-releasing neurons exert similar, quiescence-inducing effects on the animals' behavior cannot be excluded. It can, however, be concluded that this function cannot be ascribed to 5-HT neurons in general. To characterize the small 5-HT neurons of the PMPV cluster anatomically and to identify brain regions innervated by their arborizations, we used the flippase-based *Drosophila* flybow technique (Hadjieconomou et al., 2011) in combination with R66A09-Gal4. The differential expression of distinct fluorescent proteins in individual neurons covered by this Gal4 line enabled us to track and reconstruct the fine arborizations of the two small somata neurons per hemisphere (referred to here as PMPV1 and PMPV2) (Fig. 11A,B) and to compare them with a recently published nomenclature atlas of the *Drosophila* brain (Ito et al., 2014). Both neurons cross the midline but target different brain regions. Whereas PMPV1 densely innervates the superior lateral protocerebrum and shows a smaller, but finely ramified, arborization in the lamina of the optic lobe (Fig. 11A), PMPV2 innervates the superior posterior slope, the inferior bridge,
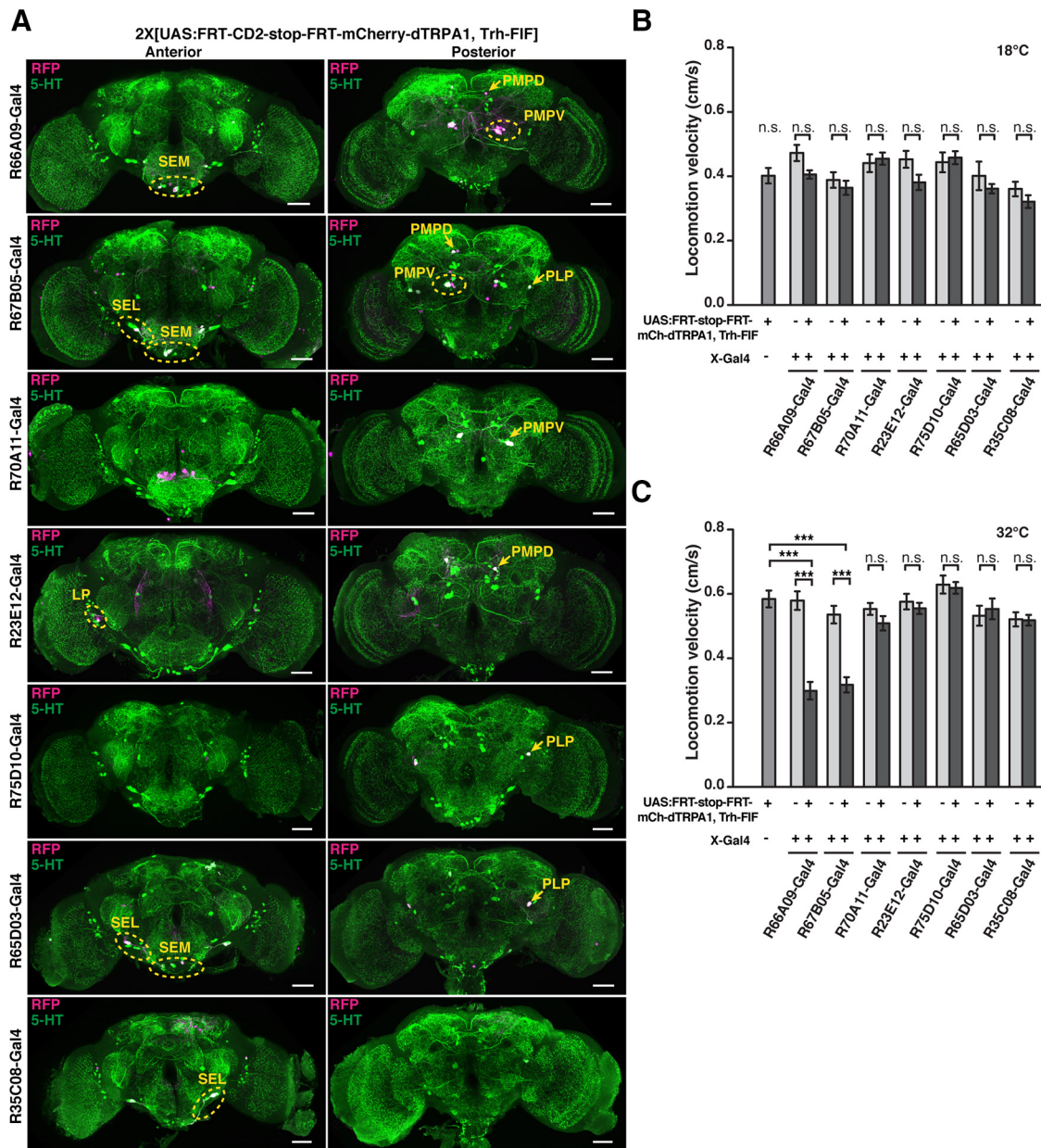
Figure 10. Thermogenetic activation of 5-HT neurons of the PMPV cluster induces behavioral quiescence. *A*, Expression of mCherry-dTRPA1 (anti-RFP immunoreactivity, magenta) in the brain under control different Gal4 driver lines (rows) is restricted to defined 5-HT neurons through a flippase (FIF) under control of a Trh-promoter sequence. Left column represents maximal intensity projections across stacks of confocal images from an anterior view on the brain. Right column represents a posterior view. Green represents anti-5-HT immunoreactivity. White represents the overlap. Yellow circles and arrows indicate identified 5-HT neuron clusters. Scale bars, 50 μm. *B*, *C*, Flies expressing mCherry-dTRPA1 in distinct subsets of 5-HT neurons and the respective parental controls were tested for locomotion velocity at 18°C (*B*) and 32°C (*C*) ($n = 26–32$). Bars indicate mean ± SEM. n.s., Not significant ($p > 0.05$). ***$p < 0.001$.

Table 5. Somata cluster designation of 5-HT neurons covered by different Gal4 driver lines and the behavioral consequence of thermogenetic activation of these neurons[a]

Gal4 lines	PMPV big	PMPV small	PMPD	SEM	SEL	PLP	Behavioral effect
R66A09	+	+	+	+	−	−	+
R67B05	+	+	+	+	+	+	+
R70A11	+	−	−	−	−	−	−
R23E12	−	−	+	−	−	−	−
R75D10	−	−	−	−	−	+	−
R65D03	−	−	−	+	+	+	−
R35C08	−	−	−	−	+	−	−

[a]Rows indicate the identity of neuronal clusters in which mCherry-dTRPA1 was expressed using different Gal4-driver strains. +, Thermogenetic activation of the indicated neurons caused a significant reduction in locomotion activity; −, thermogenetic activation of the indicated neurons did not alter locomotion activity. The combinatorial analysis reveals that locomotion activity is affected by neurons of the PMPV cluster with small somata.

and the inferior clamp (Fig. 11*B*), which are brain regions whose functions are unknown.

Distinct 5-HT-releasing neurons of the PMPV cluster affect mating, but not feeding, behavior

After having shown that distinct neurons located in the PMPV cluster are sufficient to induce behavioral quiescence defined as decreased locomotion activity, we asked whether this inactivity influences motivational behavior in general or whether the isolated PMPV neurons act selectively on distinct functional, behavioral classes (e.g., in the context of mating or feeding). We again used the intersectional gene expression approach to drive mCherry-dTRPA1 in distinct 5-HT neurons under control of R66A09-Gal4 or R67B05-Gal4. The courtship indices of wild-

A

B
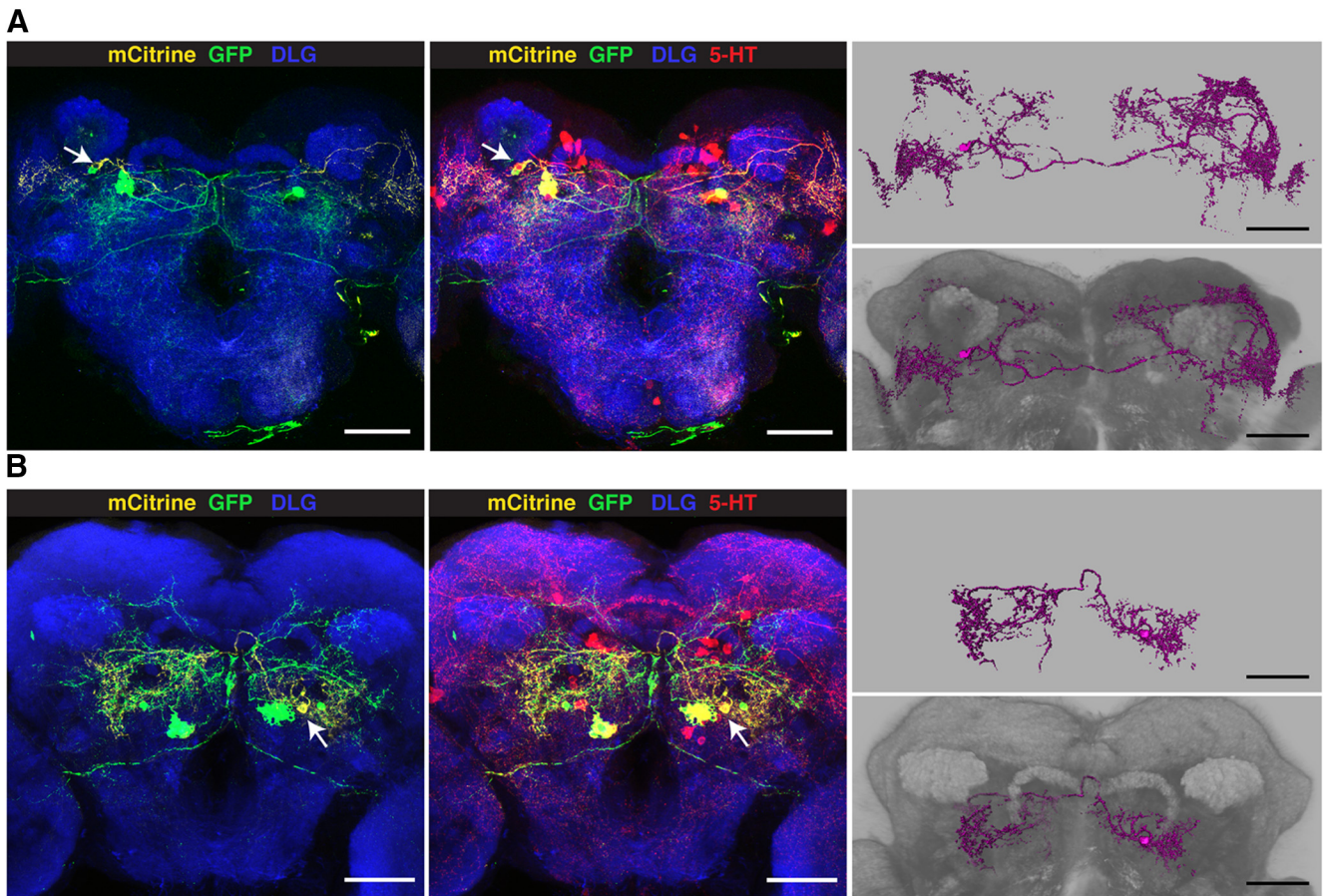
Figure 11. Anatomical description of PMPV neurons. Dense arborizations of PMPV cluster neurons were visualized by differential fluorescence reporter expression using UAS:Flybow 2.0/m-hs-FLP; R66A09-Gal4/Trh-FIF. Random expression of GFP and mCitrine in 5-HT neurons covered by R66A09-Gal4 allows for distinguishing the arborizations of two neurons, PMPV1 (**A**) and PMPV2 (**B**). Left images represent GFP (green), mCitrine (yellow) expression and anti-DLG immunoreactivity (blue). The center images show GFP and mCitrine expression overlapping with anti-5-HT immunoreactivity (red). 3D reconstructions of the two neurons are shown on the right, without (top) and with (bottom) anti-DLG staining. Scale bars, 50 μm.

type males toward females whose PMPV neurons were thermogenetically activated were unaffected ($H_{(9, N = 310)} = 26.03, p < 0.005$; Kruskal–Wallis test; pairwise *post hoc* comparisons between temperatures within genotypes: $p = 1.0$ in all cases; Fig. 12A). Their frequency of copulation attempts was also not changed significantly ($H_{(9, N = 310)} = 35.97, p < 0.001$; Kruskal–Wallis test; pairwise *post hoc* comparisons between temperatures within genotypes: $p > 0.39$). However, the males' copulation success was drastically reduced due to a decreased female receptivity (R66A09-Gal4: $p < 0.001$ for the mCherry-dTRPA1-expressing flies; $p = 0.26$ for the Gal4 line; R67B05-Gal4: $p < 0.001$ for the mCherry-dTRPA1-expressing flies; $p = 0.28$ for the Gal4 line; $p = 0.31$ for the UAS line; Fisher's exact test; Fig. 12A), just as was the case for thermogenetic activation of large populations of 5-HT neurons using Trh-Gal4 (Fig. 5A). Again, those few males that succeeded to copulate showed slightly higher latency to copulation at 29°C, but not significantly different from that at 18°C ($H_{(9, N = 173)} = 25.55, p < 0.003$; Kruskal–Wallis test; pairwise *post hoc* comparisons between temperatures within genotypes: $p = 1.0$ in all cases; Fig. 12A). Conversely, when PMPV neurons were activated in males, their courtship index was slightly, but significantly, reduced ($H_{(9, N = 310)} = 56.90, p < 0.001$; Kruskal–Wallis test; pairwise *post hoc* comparisons between temperatures within genotypes: R66A09-Gal4: $p < 0.03$ for

the mCherry-dTRPA1 expressing flies; $p = 1.0$ for the Gal4 line; R67B05-Gal4: $p < 0.04$ for the mCherry-dTRPA1 expressing flies; $p = 1.0$ for the Gal4 line; $p = 1.0$ for the UAS line; Fig. 12B). This reduction in courtship activity was not due to a decrease in all behavioral components involved in courting and mating as their wing extension frequency remained unaffected by thermoactivation of PMPV neurons ($H_{(9, N = 310)} = 43.45; p < 0.001$; Kruskal–Wallis test; pairwise *post hoc* comparisons between temperatures within genotypes: $p > 0.3$ in all cases; Fig. 12B). However, their copulation attempt frequency was significantly reduced ($H_{(9, N = 310)} = 48.62, p < 0.001$; Kruskal–Wallis test; pairwise *post hoc* comparisons between temperatures within genotypes: R66A09-Gal4: $p < 0.006$ for the mCherry-dTRPA1 expressing flies; $p = 1.0$ for the Gal4 line; R67B05-Gal4: $p < 0.002$ for the mCherry-dTRPA1 expressing flies; $p = 1.0$ for the Gal4 line; $p = 1.0$ for the UAS line). Consequently, their copulation success was likewise reduced (Fig. 12B) (R66A09-Gal4: $p < 0.001$ for the mCherry-dTRPA1-expressing flies; $p = 0.80$ for the Gal4 line; R67B05: $p < 0.001$ for the mCherry-dTRPA1-expressing flies; $p = 1.0$ for the Gal4 line; $p = 0.78$ for the UAS line; Fisher's exact test), comparable with the effect using Trh-Gal4 (Fig. 5B). Those few males that showed successful mating exhibited unaltered copulation latency ($H_{(9, N = 163)} = 8.41, p = 0.49$; Kruskal–Wallis test).
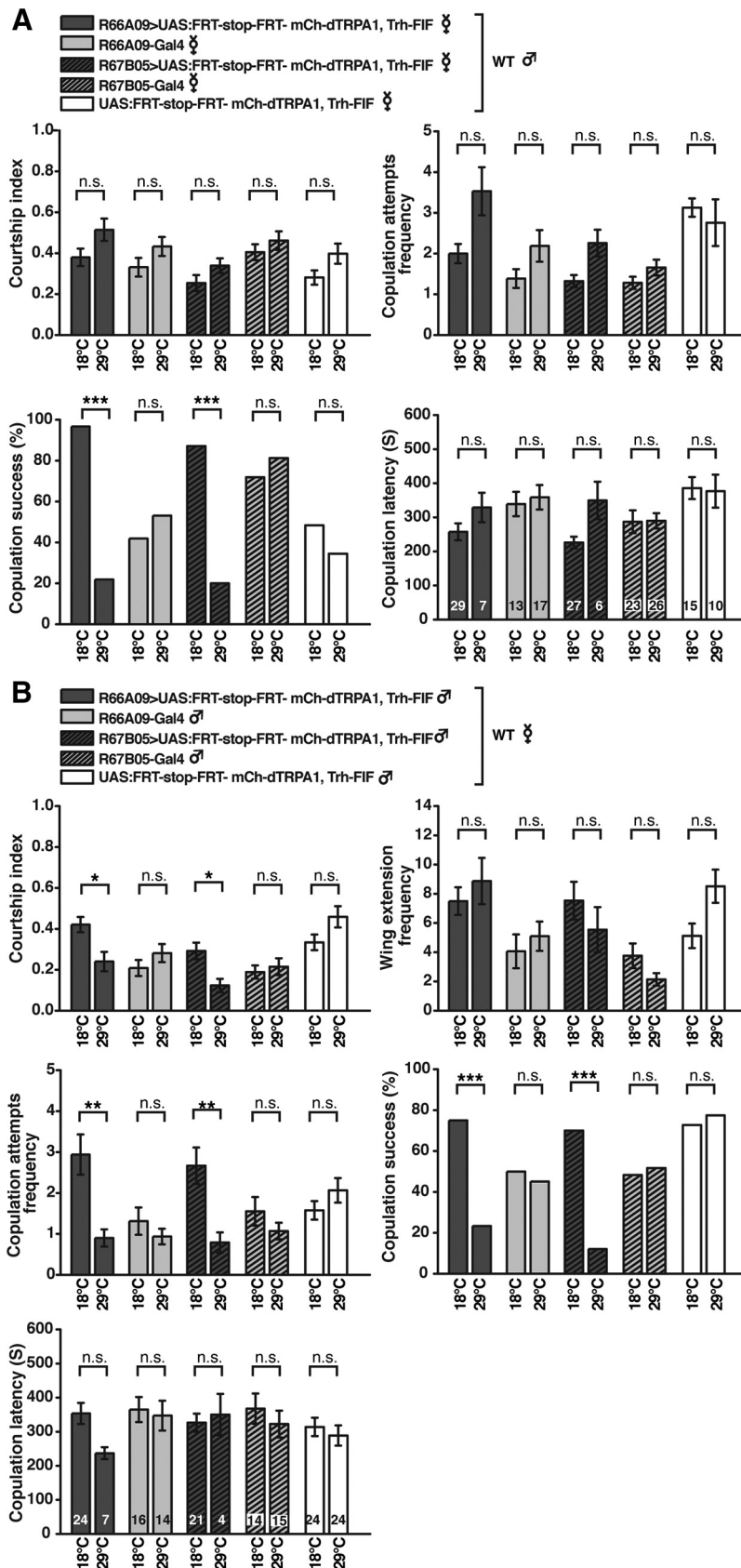
Figure 12. Thermogenetic activation of PMPV neurons affects mating behavior. *A*, Mating behavior of wild-type males toward virgin females expressing mCherry-dTRPA1 in 5-HT neurons of the PMPV cluster covered by R66A09-Gal4, R67B05-Gal4, or genetic control strains at 18°C and 29°C. For neither female genotype male courtship behavior or the frequency of copulation attempts was significantly different between 18°C and 29°C. However, copulation success (female receptivity) was significantly reduced due to

In contrast to that, food uptake remained unaffected by thermogenetic activation of 5-HT neurons covered by R66A09-Gal4 or R67B05-Gal4 (Fig. 13*A*,*B*) (18°C: $F_{(4,34)} = 2.43$, $p = 0.07$; 32°C: $F_{(4,35)} = 1.72$; $p = 0.17$; one-way ANOVA). The reduction of food uptake caused by thermogenetic activation of Trh-Gal4 (Fig. 5*C*) can, therefore, not be ascribed to neurons of the PMPV cluster. In conclusion, behavioral quiescence, as defined by lowered locomotion activity, can be mediated by few, distinct neurons of the PMPV cluster, and the majority of 5-HT neurons do not induce behavioral quiescence. However, the quiescence-inducing effect exerted by distinct 5-HT neurons of the PMPV cluster does not act as a brain-wide arousal system and does not affect motivational behavior in general. Rather, PMPV neurons influence distinct behavioral and motivational classes, such as mating, selectively.

Discussion
Counteracting roles for dopamine and serotonin in arousal?
The concept of generalized arousal assumes that animals, and the respective neuronal correlates in their brains, are in an aroused state or, conversely, a nonaroused state, with gradual transitions between the two states. In the simplest conceivable mechanistic model, one single neuromodulatory system might accomplish this task (e.g., a substance whose overall level determines the arousal state). In *Drosophila*, DA has been shown to be involved the regulation of arousal (Birman, 2005; Van Swinderen and Andretic, 2011). For example, genetic depletion of DA in the brain generally decreases arousal (Riemensperger et al., 2011), whereas increased dopamine levels achieved by a mutation in the DA transporter *dDAT* (Kume et al., 2005; Ueno et al., 2012) or by pharmacological treat-

←

thermogenetic activation of PMPV neurons. n = 29–32. Those males that succeeded to copulate showed unaltered copulation latency (*n* indicated within the bars). *B*, Mating behavior of males expressing mCherry-dTRPA1 in PMPV neurons covered by R66A09-Gal4, R67B05-Gal4, or genetic control strains toward wild-type virgin females at 18°C and 29°C. Thermogenetic activation of PMPV neurons in males significantly reduced overall courtship behavior, but not wing extension frequency. The frequency of copulation attempts and copulation success was significantly reduced (n = 30–33). Those males that succeeded to mate showed unaltered copulation latency (*n* indicated within the bars). Bars indicate means; error bars indicate SEM. n.s., Not significant (*p* > 0.05). *$p < 0.05$. **$p < 0.01$. ***$p < 0.001$.

A

B
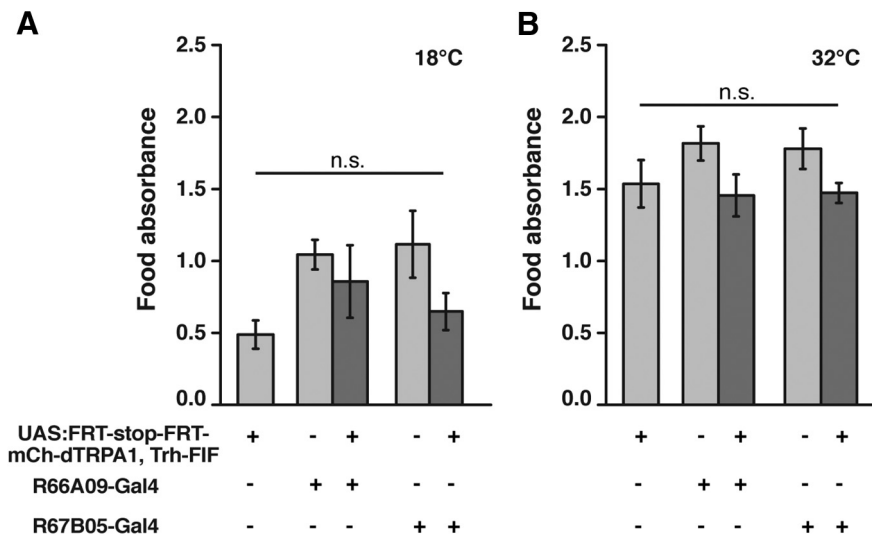
Figure 13. Food uptake is not affected by thermogenetic activation of PMPV neurons. **A, B**, Food uptake is not significantly reduced in starved flies expressing mCherry-dTRPA1 in PMPV neurons at 18°C (**A**) or 32°C (**B**) (n = 7 or 8). Bars indicate means; error bars indicate SEM. n.s., Not significant (p > 0.05).

ment (e.g., through methamphetamine) (Andretic et al., 2005), induce the opposite effect. However, studies on DA receptor mutants showed differential effects of DA on arousal in distinct circuitries (Lebestky et al., 2009). As an alternative to a potential unitary mechanism, two systems with opposite effects antagonizing each other might determine optimal arousal states. In mammals, serotonin has been considered as a general inhibitor of behavioral responses (Depue and Spoont, 1986; Spoont, 1992; Lucki, 1998), and interactions of dopaminergic and serotoninergic systems in the context of arousal have been described (Wong et al., 1995; Sasaki-Adams and Kelley, 2001; Daw et al., 2002). Impulsive aggression, for example, has been associated with hyperactivity in dopaminergic neurons and hypoactivity in serotoninergic neurons (for review, see Seo et al., 2008). Whereas in *Drosophila* the role of DA in the control of arousal is well established, the role of the 5-HT system as a potential modulator of arousal has remained less clear. In this study, we demonstrate an effect of 5-HT as a negative regulator of behavioral activity and causal element of behavioral quiescence in *Drosophila*. Thermo-activation of most 5-HT-positive cells in the brain inhibits general activity, feeding, and courtship, whereas blocking these neurons increases activity. On the one hand, motivated behavior characterized as behavior driven by internal states (e.g., hunger/appetite or reproduction-related drive) has to be terminated after the behavioral goal has been reached (e.g., through consummatory food uptake or mating). On the other hand, the execution of motivated behavior can inhibit the execution of alternative behavioral tasks. Both functions require behavior-inhibiting signals. We propose that distinct 5-HT neurons in combination with behavior-facilitating modulatory systems (e.g., DA) contribute to orchestrate the initiation and termination of selective behaviors.

Is there a "serotonin system?"
Serotonin is involved in an overwhelming plethora of simple and complex behaviors and physiological functions, both in mammals and insects, although it is released by relatively small numbers of neurons compared with those in their target areas (Cools et al., 2008; Blenau and Thamm, 2011). Accordingly, impairments in 5-HT signaling in mammals result in complex and very

diverse diseases (e.g., mood disorders, stress and anxiety disorders, or eating disorders) (Hildebrandt et al., 2010; Hale et al., 2012). Although insect behavior does not bear similarly complex psychological implications, *Drosophila*'s behavioral repertoire is rich and, in many aspects, dependent on proper 5-HT signaling. In larval or adult *Drosophila*, 5-HT has been shown to affect feeding behavior (Neckameyer, 2010; Gasque et al., 2013), courtship behavior (Becnel et al., 2011), aggression (Dierick and Greenspan, 2007; Alekseyenko et al., 2010, 2014), and memory formation (Sitaraman et al., 2008, 2012; Lee et al., 2011). Understanding this complexity is made difficult by both the widespread arborizations of 5-HT neurons and the relatively large number of 5-HT receptor genes (i.e., at least 14 in mammals) (Hannon and Hoyer, 2008) and five in *Drosophila* (Blenau and Thamm, 2011). Our knowledge about the behavioral and physiological roles of 5-HT in both *Drosophila* and mammals derives mainly from studies using brain-wide, global manipulations of 5-HT or its target (e.g., by pharmacological or genetic block of its synthesis) (Dierick and Greenspan, 2007; Sitaraman et al., 2008; Neckameyer, 2010; Lee et al., 2011; Sadaf et al., 2012), or by pharmacological or genetic impairment of 5-HT receptors (Yuan et al., 2005, 2006; Nichols, 2007; Becnel et al., 2011; Gasque et al., 2013), as well as by manipulating 5-HT reuptake through transporters (Silva et al., 2014). However, in recent years, the development of elaborate techniques to selectively dissect neuronal circuits in a cell-specific manner in model systems like *Drosophila* has advanced strongly (Venken et al., 2011), paving the way for the attribution of more precise roles to subpopulations of distinct, identifiable neurons. In the context of arousal, cells of two different subpopulations of dopaminergic neurons, PPL1 and PPM3 clusters, projecting to the dorsal fan-shaped body of the central complex, have been identified as being sufficient to promote wakefulness (Liu et al., 2012b; Ueno et al., 2012). Here, we have designed a two-step approach (i.e., stochastic targeting of 5-HT neurons followed by an intersectional strategy) to dissect and identify subsets of 5-HT neurons underlying the modulation of behavior. We identified a subset of 5-HT neurons whose activation is sufficient to induce behavioral quiescence. Although functional redundancy or synergistic effects of other 5-HT neurons cannot be excluded, the majority of 5-HT neurons are not sufficient to induce such behavioral quiescence. This suggests that 5-HT-producing cells do not act as a homogeneous and global "serotonin system" and therefore do not represent a unitary negative "arousal system." Rather, distinct 5-HT neurons are differentially involved in diverse behavioral tasks. Indeed, a single pair of 5-HT neurons located in the posterior lateral protocerebrum cluster has recently been isolated, the activity of which causes an escalation of aggression (Alekseyenko et al., 2014). Serotoninergic DPM neurons innervating the mushroom bodies are required for associative olfactory memory consolidation (Lee et al., 2011) and act as sleep-promoting neurons (Haynes et al., 2015). It has been suggested that other 5-HT neurons innervating the antennal lobes (Roy et al., 2007) modulate sensory and olfactory processing (Dacks et al., 2009). Here we show that two pairs of 5-HT neurons located in the PMPV cluster

are sufficient to induce behavioral quiescence in terms of decreased locomotor activity but do not exert their effects on all aspects of behavior. Whereas male copulation behavior, but not all aspects of courtship behavior in general, and female receptivity are reduced, feeding behavior remains unperturbed. One of the neurons identified in the PMPV cluster, PMPV1, densely innervates the superior lateral protocerebrum. Interestingly, two other types of neurons project to this brain region as well: a subset of fruitless-expressing interneurons (mAL), which show a sexual dimorphism in numbers and arborization patterns (Kimura et al., 2005), and some groups of mushroom body output neurons (Aso et al., 2014). In the superior lateral protocerebrum region, these neurons might be modulated by PMPV1 neurons, ultimately regulating courtship behavior. We find feeding behavior also to be affected by thermogenetically activating a large proportion of 5-HT neurons, in accordance with pharmacological findings (Gasque et al., 2013), but not by those PMPV cluster neurons that we isolated. Because our approach to identify neurons is based on monitoring locomotor activity, it might be that feeding-regulating 5-HT neurons are not directly associated with locomotor behavior. Alternatively, PMPV cluster neurons that we did not analyze in detail or neurons from other clusters that escaped our stochastic analysis modulate this type of behavior. It would be interesting to further dissect the remaining neurons of the PMPV cluster in the future and to test whether they affect other behavioral modules selectively, depending on their target areas. Overall, our findings strengthen the idea that modulatory, biogenic amines do not coordinate behavior as unitary, central systems. Rather, our data provide further evidence that few, distinct 5-HT neurons modulate specialized neuronal circuits responsible for distinct behavioral tasks.

References

Alekseyenko OV, Lee C, Kravitz EA (2010) Targeted manipulation of serotonergic neurotransmission affects the escalation of aggression in adult male *Drosophila melanogaster*. PLoS One 5:e10806. CrossRef Medline

Alekseyenko OV, Chan YB, Fernandez Mde L, Bülow T, Pankratz MJ, Kravitz EA (2014) Single serotonergic neurons that modulate aggression in *Drosophila*. Curr Biol 24:2700–2707. CrossRef Medline

Andretic R, van Swinderen B, Greenspan RJ (2005) Dopaminergic modulation of arousal in *Drosophila*. Curr Biol 15:1165–1175. CrossRef Medline

Andrew RJ (1974) Arousal and the causation of behaviour. Behaviour 51:135–165. CrossRef Medline

Aso Y, Hattori D, Yu Y, Johnston RM, Iyer NA, Ngo TT, Dionne H, Abbott LF, Axel R, Tanimoto H, Rubin GM (2014) The neuronal architecture of the mushroom body provides a logic for associative learning. ELife 3:e04577. CrossRef Medline

Basler K, Struhl G (1994) Compartment boundaries and the control of *Drosophila* limb pattern by hedgehog protein. Nature 368:208–214. CrossRef Medline

Becnel J, Johnson O, Luo J, Nässel DR, Nichols CD (2011) The serotonin 5-HT7Dro receptor is expressed in the brain of *Drosophila*, and is essential for normal courtship and mating. PLoS One 6:e20800. CrossRef Medline

Benzer S (1967) Behavioral mutants of *Drosophila* isolated by countercurrent distribution. Proc Natl Acad Sci U S A 58:1112–1119. CrossRef Medline

Bianchi D, Marasco A, Limongiello A, Marchetti C, Marie H, Tirozzi B, Migliore M (2012) On the mechanisms underlying the depolarization block in the spiking dynamics of CA1 pyramidal neurons. J Comput Neurosci 33:207–225. CrossRef Medline

Birman S (2005) Arousal mechanisms: speedy flies don't sleep at night. Curr Biol 15:R511–R513. CrossRef Medline

Blenau W, Thamm M (2011) Distribution of serotonin (5-HT) and its receptors in the insect brain with focus on the mushroom bodies: lessons from *Drosophila melanogaster* and *Apis mellifera*. Arthropod Struct Dev 40:381–394. CrossRef Medline

Bohm RA, Welch WP, Goodnight LK, Cox LW, Henry LG, Gunter TC, Bao H,

Zhang B (2010) A genetic mosaic approach for neural circuit mapping in *Drosophila*. Proc Natl Acad Sci U S A 107:16378–16383. CrossRef Medline

Brand AH, Perrimon N (1993) Targeted gene expression as a means of altering cell fates and generating dominant phenotypes. Development 118:401–415. Medline

Brown RE, Basheer R, McKenna JT, Strecker RE, McCarley RW (2012) Control of sleep and wakefulness. Physiol Rev 92:1087–1187. CrossRef Medline

Clyne JD, Miesenböck G (2008) Sex-specific control and tuning of the pattern generator for courtship song in *Drosophila*. Cell 133:354–363. CrossRef Medline

Coleman CM, Neckameyer WS (2005) Serotonin synthesis by two distinct enzymes in *Drosophila melanogaster*. Arch Insect Biochem Physiol 59:12–31. CrossRef Medline

Cools R, Roberts AC, Robbins TW (2008) Serotoninergic regulation of emotional and behavioural control processes. Trends Cogn Sci 12:31–40. CrossRef Medline

Coull JT (1998) Neural correlates of attention and arousal: insights from electrophysiology, functional neuroimaging and psychopharmacology. Prog Neurobiol 55:343–361. CrossRef Medline

Crocker A, Shahidullah M, Levitan IB, Sehgal A (2010) Identification of a neural circuit that underlies the effects of octopamine on sleep:wake behavior. Neuron 65:670–681. CrossRef Medline

Dacks AM, Green DS, Root CM, Nighorn AJ, Wang JW (2009) Serotonin modulates olfactory processing in the antennal lobe of *Drosophila*. J Neurogenet 23:366–377. CrossRef Medline

Dasari S, Viele K, Turner AC, Cooper RL (2007) Influence of PCPA and MDMA (ecstasy) on physiology, development and behavior in *Drosophila melanogaster*. Eur J Neurosci 26:424–438. CrossRef Medline

Daw ND, Kakade S, Dayan P (2002) Opponent interactions between serotonin and dopamine. Neural Netw 15:603–616. CrossRef Medline

Depue RA, Spoont MR (1986) Conceptualizing a serotonin trait: a behavioral dimension of constraint. Ann N Y Acad Sci 487:47–62. CrossRef Medline

Dierick HA, Greenspan RJ (2007) Serotonin and neuropeptide F have opposite modulatory effects on fly aggression. Nat Genet 39:678–682. CrossRef Medline

Dietzl G, Chen D, Schnorrer F, Su KC, Barinova Y, Fellner M, Gasser B, Kinsey K, Oppel S, Scheiblauer S, Couto A, Marra V, Keleman K, Dickson BJ (2007) A genome-wide transgenic RNAi library for conditional gene inactivation in *Drosophila*. Nature 448:151–156. CrossRef Medline

Gasque G, Conway S, Huang J, Rao Y, Vosshall LB (2013) Small molecule drug screening in *Drosophila* identifies the 5HT2A receptor as a feeding modulation target. Sci Rep 3:srep02120. CrossRef Medline

Hadjieconomou D, Rotkopf S, Alexandre C, Bell DM, Dickson BJ, Salecker I (2011) Flybow: genetic multicolor cell labeling for neural circuit analysis in *Drosophila melanogaster*. Nat Methods 8:260–266. CrossRef Medline

Hale MW, Shekhar A, Lowry CA (2012) Stress-related serotonergic systems: implications for symptomatology of anxiety and affective disorders. Cell Mol Neurobiol 32:695–708. CrossRef Medline

Hamada FN, Rosenzweig M, Kang K, Pulver SR, Ghezzi A, Jegla TJ, Garrity PA (2008) An internal thermal sensor controlling temperature preference in *Drosophila*. Nature 454:217–220. CrossRef Medline

Hannon J, Hoyer D (2008) Molecular biology of 5-HT receptors. Behav Brain Res 195:198–213. CrossRef Medline

Haynes PR, Christmann BL, Griffith LC (2015) A single pair of neurons links sleep to memory consolidation in *Drosophila melanogaster*. eLife Sci e03868.

Hebb DO (1955) Drives and the C.N.S. (conceptual nervous system). Psychol Rev 62:243–254. CrossRef Medline

Hildebrandt T, Alfano L, Tricamo M, Pfaff DW (2010) Conceptualizing the role of estrogens and serotonin in the development and maintenance of bulimia nervosa. Clin Psychol Rev 30:655–668. CrossRef Medline

Inagaki HK, Kamikouchi A, Ito K (2010) Methods for quantifying simple gravity sensing in *Drosophila melanogaster*. Nat Protoc 5:20–25. CrossRef Medline

Ito K, Shinomiya K, Ito M, Armstrong JD, Boyan G, Hartenstein V, Harzsch S, Heisenberg M, Homberg U, Jenett A, Keshishian H, Restifo LL, Rössler W, Simpson JH, Strausfeld NJ, Strauss R, Vosshall LB, Insect Brain Name

Working Group (2014) A systematic nomenclature for the insect brain. Neuron 81:755–765. CrossRef Medline

Jenett A, Rubin GM, Ngo TT, Shepherd D, Murphy C, Dionne H, Pfeiffer BD, Cavallaro A, Hall D, Jeter J, Iyer N, Fetter D, Hausenfluck JH, Peng H, Trautman ET, Svirskas RR, Myers EW, Iwinski ZR, Aso Y, DePasquale GM, et al. (2012) A GAL4-driver line resource for *Drosophila* neurobiology. Cell Rep 2:991–1001. CrossRef Medline

Jing J, Gillette R, Weiss KR (2009) Evolving concepts of arousal: insights from simple model systems. Rev Neurosci 20:405–427. Medline

Kimura K, Ote M, Tazawa T, Yamamoto D (2005) Fruitless specifies sexually dimorphic neural circuitry in the *Drosophila* brain. Nature 438:229–233. CrossRef Medline

Kitamoto T (2001) Conditional modification of behavior in *Drosophila* by targeted expression of a temperature-sensitive shibire allele in defined neurons. J Neurobiol 47:81–92. CrossRef Medline

Koe BK, Weissman A (1966) p-Chlorophenylalanine: a specific depletor of brain serotonin. J Pharmacol Exp Ther 154:499–516. Medline

Kume K, Kume S, Park SK, Hirsh J, Jackson FR (2005) Dopamine is a regulator of arousal in the fruit fly. J Neurosci 25:7377–7384. CrossRef Medline

Lebestky T, Chang JS, Dankert H, Zelnik L, Kim YC, Han KA, Wolf FW, Perona P, Anderson DJ (2009) Two different forms of arousal in *Drosophila* are oppositely regulated by the dopamine D1 receptor ortholog DopR via distinct neural circuits. Neuron 64:522–536. CrossRef Medline

Lee PT, Lin HW, Chang YH, Fu TF, Dubnau J, Hirsh J, Lee T, Chiang AS (2011) Serotonin-mushroom body circuit modulating the formation of anesthesia-resistant memory in *Drosophila*. Proc Natl Acad Sci U S A 108:13794–13799. CrossRef Medline

Li H, Chaney S, Roberts IJ, Forte M, Hirsh J (2000) Ectopic G-protein expression in dopamine and serotonin neurons blocks cocaine sensitization in *Drosophila melanogaster*. Curr Biol 10:211–214. CrossRef Medline

Liu C, Plaçais PY, Yamagata N, Pfeiffer BD, Aso Y, Friedrich AB, Siwanowicz I, Rubin GM, Preat T, Tanimoto H (2012a) A subset of dopamine neurons signals reward for odour memory in *Drosophila*. Nature 488:512–516. CrossRef Medline

Liu Q, Liu S, Kodama L, Driscoll MR, Wu MN (2012b) Two dopaminergic neurons signal to the dorsal fan-shaped body to promote wakefulness in *Drosophila*. Curr Biol 22:2114–2123. CrossRef Medline

Lucki I (1998) The spectrum of behaviors influenced by serotonin. Biol Psychiatry 44:151–162. CrossRef Medline

Nall A, Sehgal A (2014) Monoamines and sleep in *Drosophila*. Behav Neurosci 128:264–272. CrossRef Medline

Neckameyer WS (2010) A trophic role for serotonin in the development of a simple feeding circuit. Dev Neurosci 32:217–237. CrossRef Medline

Neckameyer WS, Coleman CM, Eadie S, Goodwin SF (2007) Compartmentalization of neuronal and peripheral serotonin synthesis in *Drosophila melanogaster*. Genes Brain Behav 6:756–769. CrossRef Medline

Ni JQ, Liu LP, Binari R, Hardy R, Shim HS, Cavallaro A, Booker M, Pfeiffer BD, Markstein M, Wang H, Villalta C, Laverty TR, Perkins LA, Perrimon N (2009) A *Drosophila* resource of transgenic RNAi lines for neurogenetics. Genetics 182:1089–1100. CrossRef Medline

Nichols CD (2007) 5-HT2 receptors in *Drosophila* are expressed in the brain and modulate aspects of circadian behaviors. Dev Neurobiol 67:752–763. CrossRef Medline

Park J, Lee SB, Lee S, Kim Y, Song S, Kim S, Bae E, Kim J, Shong M, Kim JM, Chung J (2006) Mitochondrial dysfunction in *Drosophila* PINK1 mutants is complemented by parkin. Nature 441:1157–1161. CrossRef Medline

Parkes TL, Elia AJ, Dickinson D, Hilliker AJ, Phillips JP, Boulianne GL (1998) Extension of *Drosophila* lifespan by overexpression of human SOD1 in motorneurons. Nat Genet 19:171–174. CrossRef Medline

Pech U, Pooryasin A, Birman S, Fiala A (2013) Localization of the contacts between Kenyon cells and aminergic neurons in the *Drosophila melanogaster* brain using SplitGFP reconstitution. J Comp Neurol 521:3992–4026. CrossRef Medline

Pfaff D, Ribeiro A, Matthews J, Kow LM (2008) Concepts and mechanisms of generalized central nervous system arousal. Ann N Y Acad Sci 1129:11–25. CrossRef Medline

Pfeiffenberger C, Lear BC, Keegan KP, Allada R (2010) Locomotor activity level monitoring using the *Drosophila* Activity Monitoring (DAM) System. Cold Spring Harb Protoc 2010:pdb.prot5518. Medline

Pfeiffer BD, Jenett A, Hammonds AS, Ngo TT, Misra S, Murphy C, Scully A, Carlson JW, Wan KH, Laverty TR, Mungall C, Svirskas R, Kadonaga JT, Doe CQ, Eisen MB, Celniker SE, Rubin GM (2008) Tools for neuroanatomy and neurogenetics in *Drosophila*. Proc Natl Acad Sci U S A 105:9715–9720. CrossRef Medline

Pfeiffer BD, Ngo TT, Hibbard KL, Murphy C, Jenett A, Truman JW, Rubin GM (2010) Refinement of tools for targeted gene expression in *Drosophila*. Genetics 186:735–755. CrossRef Medline

Pfeiffer BD, Truman JW, Rubin GM (2012) Using translational enhancers to increase transgene expression in *Drosophila*. Proc Natl Acad Sci U S A 109:6626–6631. CrossRef Medline

Pignoni F, Zipursky SL (1997) Induction of *Drosophila* eye development by decapentaplegic. Development 124:271–278. Medline

Riemensperger T, Isabel G, Coulom H, Neuser K, Seugnet L, Kume K, Iché-Torres M, Cassar M, Strauss R, Preat T, Hirsh J, Birman S (2011) Behavioral consequences of dopamine deficiency in the *Drosophila* central nervous system. Proc Natl Acad Sci U S A 108:834–839. CrossRef Medline

Roy B, Singh AP, Shetty C, Chaudhary V, North A, Landgraf M, Vijayraghavan K, Rodrigues V (2007) Metamorphosis of an identified serotonergic neuron in the *Drosophila* olfactory system. Neural Dev 2:20. CrossRef Medline

Sadaf S, Birman S, Hasan G (2012) Synaptic activity in serotonergic neurons is required for air-puff stimulated flight in *Drosophila melanogaster*. PLoS One 7:e46405. CrossRef Medline

Sasaki-Adams DM, Kelley AE (2001) Serotonin-dopamine interactions in the control of conditioned reinforcement and motor behavior. Neuropsychopharmacology 25:440–452. CrossRef Medline

Schindelin J, Arganda-Carreras I, Frise E, Kaynig V, Longair M, Pietzsch T, Preibisch S, Rueden C, Saalfeld S, Schmid B, Tinevez JY, White DJ, Hartenstein V, Eliceiri K, Tomancak P, Cardona A (2012) Fiji: an open-source platform for biological-image analysis. Nat Methods 9:676–682. CrossRef Medline

Seo D, Patrick CJ, Kennealy PJ (2008) Role of serotonin and dopamine system interactions in the neurobiology of impulsive aggression and its comorbidity with other clinical disorders. Aggress Violent Behav 13:383–395. CrossRef Medline

Shaw PJ, Cirelli C, Greenspan RJ, Tononi G (2000) Correlates of sleep and waking in *Drosophila melanogaster*. Science 287:1834–1837. CrossRef Medline

Shimosako N, Hadjieconomou D, Salecker I (2014) Flybow to dissect circuit assembly in the *Drosophila* brain. Methods Mol Biol 1082:57–69. CrossRef Medline

Shiraiwa T, Carlson JR (2007) Proboscis extension response (PER) assay in *Drosophila*. J Vis Exp 3:193. CrossRef Medline

Siegel RW, Hall JC (1979) Conditioned responses in courtship behavior of normal and mutant *Drosophila*. Proc Natl Acad Sci U S A 76:3430–3434. CrossRef Medline

Silva B, Goles NI, Varas R, Campusano JM (2014) Serotonin receptors expressed in *Drosophila* mushroom bodies differentially modulate larval locomotion. PLoS One 9:e89641. CrossRef Medline

Sitaraman D, Zars M, Laferriere H, Chen YC, Sable-Smith A, Kitamoto T, Rottinghaus GE, Zars T (2008) Serotonin is necessary for place memory in *Drosophila*. Proc Natl Acad Sci U S A 105:5579–5584. CrossRef Medline

Sitaraman D, LaFerriere H, Birman S, Zars T (2012) Serotonin is critical for rewarded olfactory short-term memory in *Drosophila*. J Neurogenet 26:238–244. CrossRef Medline

Spoont MR (1992) Modulatory role of serotonin in neural information processing: implications for human psychopathology. Psychol Bull 112:330–350. CrossRef Medline

Thum AS, Knapek S, Rister J, Dierichs-Schmitt E, Heisenberg M, Tanimoto H (2006) Differential potencies of effector genes in adult *Drosophila*. J Comp Neurol 498:194–203. CrossRef Medline

Ueno T, Tomita J, Tanimoto H, Endo K, Ito K, Kume S, Kume K (2012) Identification of a dopamine pathway that regulates sleep and arousal in *Drosophila*. Nat Neurosci 15:1516–1523. CrossRef Medline

Vallés AM, White K (1988) Serotonin-containing neurons in *Drosophila melanogaster*: development and distribution. J Comp Neurol 268:414–428. CrossRef Medline

Van Swinderen B, Andretic R (2011) Dopamine in *Drosophila*: setting arousal thresholds in a miniature brain. Proc Biol Sci 278:906–913. CrossRef Medline

Vasmer D, Pooryasin A, Riemensperger T, Fiala A (2014) Induction of aversive learning through thermogenetic activation of Kenyon cell ensembles in *Drosophila*. Front Behav Neurosci 8:174. CrossRef Medline

Venken KJ, Simpson JH, Bellen HJ (2011) Genetic manipulation of genes and cells in the nervous system of the fruit fly. Neuron 72:202–230. CrossRef Medline

Wagh DA, Rasse TM, Asan E, Hofbauer A, Schwenkert I, Dürrbeck H, Buchner S, Dabauvalle MC, Schmidt M, Qin G, Wichmann C, Kittel R, Sigrist SJ, Buchner E (2006) Bruchpilot, a protein with homology to ELKS/CAST, is required for structural integrity and function of synaptic active zones in *Drosophila*. Neuron 49:833–844. CrossRef Medline

Wong PT, Feng H, Teo WL (1995) Interaction of the dopaminergic and serotonergic systems in the rat striatum: effects of selective antagonists and uptake inhibitors. Neurosci Res 23:115–119. CrossRef Medline

Yu JY, Kanai MI, Demir E, Jefferis GS, Dickson BJ (2010) Cellular organization of the neural circuit that drives *Drosophila* courtship behavior. Curr Biol 20:1602–1614. CrossRef Medline

Yuan Q, Lin F, Zheng X, Sehgal A (2005) Serotonin modulates circadian entrainment in *Drosophila*. Neuron 47:115–127. CrossRef Medline

Yuan Q, Joiner WJ, Sehgal A (2006) A sleep-promoting role for the *Drosophila* serotonin receptor 1A. Curr Biol 16:1051–1062. CrossRef Medline